

Inference-Time Alignment in Diffusion Models with Reward-Guided Generation: Tutorial and Review

Masatoshi Uehara ^{1*}, Yulai Zhao ², Chenyu Wang ³, Xiner Li ⁴,

Aviv Regev ¹, Sergey Levine ^{5*}, Tommaso Biancalani ^{1*}

¹Genentech, ²Princeton University, ³MIT,
⁴Texas A&M University, ⁵UC Berkeley

Abstract

This tutorial provides an in-depth guide on inference-time guidance and alignment methods for optimizing downstream reward functions in diffusion models. While diffusion models are renowned for their generative modeling capabilities, practical applications in fields such as biology often require sample generation that maximizes specific metrics (e.g., stability, affinity in proteins, closeness to target structures). In these scenarios, diffusion models can be adapted not only to generate realistic samples but also to explicitly maximize desired measures at inference time without fine-tuning. This tutorial explores the foundational aspects of such inference-time algorithms. We review these methods from a unified perspective, demonstrating that current techniques—such as Sequential Monte Carlo (SMC)-based guidance, value-based importance sampling, and classifier guidance—aim to approximate soft optimal denoising processes (a.k.a. policies in RL) that combine pre-trained denoising processes with value functions serving as look-ahead functions that predict from intermediate states to terminal rewards. Within this framework, we present several novel algorithms not yet covered in the literature. Furthermore, we discuss (1) fine-tuning methods combined with inference-time techniques, (2) inference-time algorithms based on search algorithms, which have received limited attention in current research, and (3) connections between inference-time algorithms in language models and diffusion models. The code of this tutorial on protein design is available at <https://github.com/masa-ue/AlignInversePro>.

Keyword: *Diffusion Models, Test-Time Alignment, Reinforcement Learning, Classifier Guidance, Sequential Monte Carlo, Model-Based Optimization, Tree Search, Protein Design*

*ueharamasatoshi136@gmail.com

Introduction

Diffusion models (Sohl-Dickstein et al., 2015; Ho et al., 2020; Song et al., 2020) have demonstrated remarkable success in computer vision, particularly as generative models for continuous domains such as images (Rombach et al., 2022). This success has been further extended to scientific areas such as the generation of protein 3D structures (Yim et al., 2023; Watson et al., 2023; Chu et al., 2024; Abramson et al., 2024) and small molecule 3D structures (Xu et al., 2022; Jing et al., 2022; Corso et al., 2022). Furthermore, recent works (Shi et al., 2024; Sahoo et al., 2024; Lou et al., 2023) have shown promising results with diffusion over traditional autoregressive models in *discrete* domains. Building on this progress in natural language processing (NLP), the use of diffusion models has also been explored for generating biological sequences (proteins, RNA, and DNA), which are inherently non-causal, because these sequences fold into complex tertiary (3D) structures (Campbell et al., 2024; Sarkar et al., 2024; Winnifrieth et al., 2024; Wang et al., 2024).

Controlled generation is a pivotal topic in the study of diffusion models. In the context of “foundational models”, the process typically begins with training conditional diffusion models on large datasets to generate natural designs (e.g., biologically plausible protein sequences) conditioned on fundamental functionalities. Following this pre-training stage, the focus often shifts to optimizing specific downstream reward functions, commonly referred to as “alignment” problems in AI. By guiding generation to maximize a given reward during inference (e.g., binding affinity or stability in protein sequences), diffusion models can be effectively utilized as robust computational design frameworks. Similarly, conditioning on target properties during inference is treated as a reward maximization task, where rewards are frequently defined using classifiers.

In this tutorial, we aim to explore inference-time techniques for controlled generation in diffusion models, along with their foundational properties. These techniques aim to seamlessly integrate pre-trained generative models trained on large-scale datasets with reward models, as illustrated in Figure 1. Specifically, at each generation step in pre-trained diffusion models, certain modifications are introduced to optimize downstream reward functions as summarized in Figure 2. A significant advantage of these methods is that they don’t require post-training of the diffusion models, which can be computationally demanding. The simplest such approach is best-of-N sampling in Figure 2a, which involves generating multiple designs (N samples) from a pre-trained diffusion model and selecting the best one based on reward

functions (e.g., Nakano et al. (2021)). However, this method can be highly inefficient when the reward functions are difficult to optimize. More efficient sophisticated strategies include classifier guidance in Figure 2b and its variants (Dhariwal and Nichol, 2021; Song et al., 2021), sequential

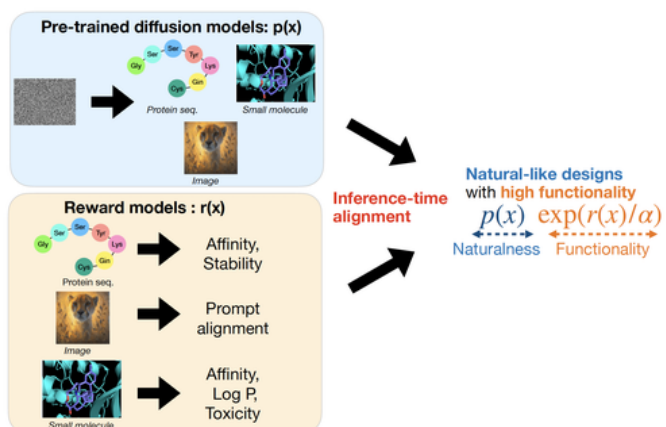


Figure 1: The objective of inference-time techniques is to generate natural designs (e.g., natural images or natural-like protein sequences) with high functionality, without any direct fine-tuning of diffusion models.

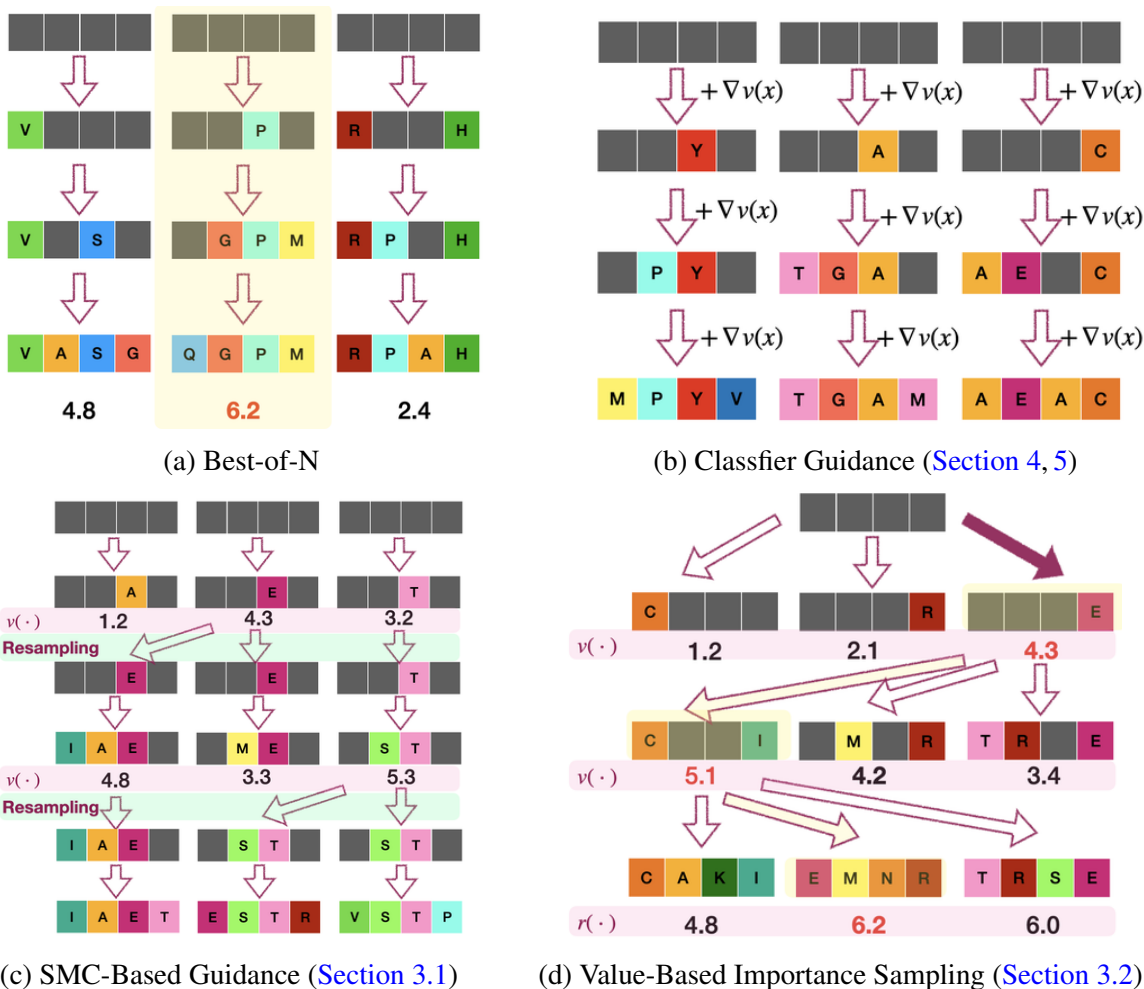
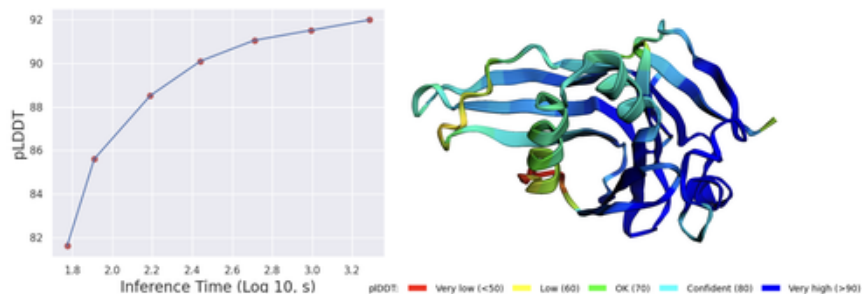


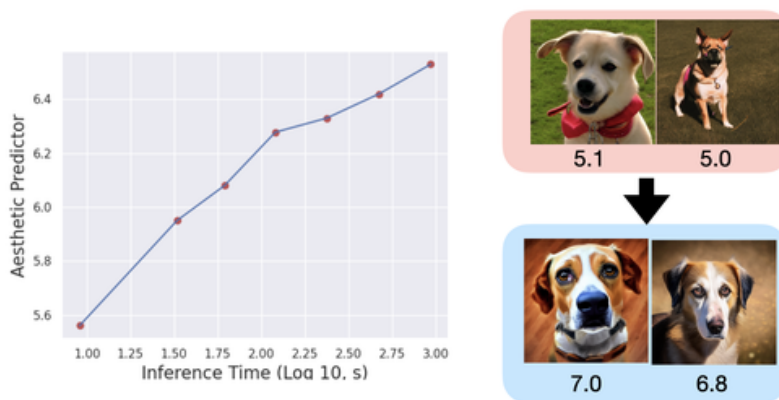
Figure 2: Summary of representative inference-time algorithms. Here, we aim to optimize downstream reward functions $r : \mathcal{X} \rightarrow \mathbb{R}$ given pre-trained masked diffusion models for sequences. The value function $v(\cdot)$ serves as a look-ahead function, mapping intermediate states to expected future rewards $r(\cdot)$. Best-of-N is a naïve method that selects the best sample among N generated ones. Derivative-based guidance adds gradients of differentiable value function models during inference, making it a powerful method when we can construct the actual value function models. SMC-Based Guidance and Value-Based Importance Sampling (a.k.a. beam search with value functions) are gradient-free methods that sequentially select favorable intermediate states based on value functions. These methods do not require constructing differentiable value function models, which can often be challenging in molecular design.

Monte Carlo-based methods in Figure 2c (Wu et al., 2024; Dou and Song, 2024; Cardoso et al., 2023; Phillips et al., 2024), and value-based sampling methods in Figure 2d (Li et al., 2024).

Before delving into the details of inference-time techniques, we provide a brief overview of this tutorial in the introduction. We begin by emphasizing the advantages of inference-time methods over post-training approaches, which can also enable controlled generation. Next, we outline the key components essential for inference-time controlled generation. Finally, we offer a comprehensive overview of the inference-time techniques covered in this work.



(a) The Y-axis represents the mean pLDDT across residues, which is a common computational proxy for stability derived from AlphaFold2, as noted in Dauparas et al. (2022); Ye et al. (2024); Ahdritz et al. (2024)



(b) LAION Aesthetic Predictor V2 (Schuhmann, 2022) serves as a typical proxy for aesthetic scores. For instance, in the figure on the right, the scores correspond to images in pink generated by the pre-trained diffusion model (Stable Diffusion in Podell et al. (2023)), while the scores correspond to images in blue obtained using inference-time techniques.

Figure 3: Scaling inference time compute via value-based beam search (Li et al., 2024) in Section 3.4, progressively increasing the tree width (see Figure 2d). These figures demonstrate that as the computational budget (x-axis) increases, rewards (y-axis) can be optimized more effectively.

Inference-Time Techniques vs. Post-Training

After pre-training, there are two main approaches for controlled generation: inference-time techniques (i.e., without fine-tuning diffusion models) and post-training methods such as RL-based fine-tuning (Black et al., 2023; Fan et al., 2023; Clark et al., 2023; Uehara et al., 2024) or classifier-free guidance-based fine-tuning (Ho and Salimans, 2022; Zhang et al., 2023; Yuan et al., 2024). In this work, we focus on reviewing the former. For a comprehensive overview of the latter approach, we refer readers to Uehara et al. (2024). While both approaches are important, inference-time techniques generally offer several advantages:

- Inference-time techniques are particularly *straightforward to implement*, as many of these methods are not only *fine-tuning-free* but also *training-free*, given access to reward functions. Despite their simplicity, they could deliver competitive performance compared to RL-based fine-tuning approaches. Indeed, for example, we can effectively optimize downstream rewards

without any fine-tuning by increasing the computational budget, as illustrated in [Figure 3](#). This scaling approach has recently been further explored in [Singhal et al. \(2025\)](#); [Ma et al. \(2025\)](#).

- *Inference-time techniques can support post-training.* For example, they can be employed as data augmentation methods within classifier-free guidance or as teacher policies in policy distillation-based post-training. Further details are provided in [Section 9.4](#).
- Even after obtaining fine-tuned models through post-training techniques, applying inference-time methods to fine-tune models can be advantageous for further improving the functionality of the generated outputs. This is particularly relevant when downstream reward feedback is highly accurate. Post-training may not fully exploit the information provided by the reward feedback, as it involves converting this feedback into data, a process that can result in information loss. In contrast, inference-time techniques can directly utilize reward feedback without the need for such conversion, enabling more effective optimization.

Critical Considerations for Choosing Inference-Time Techniques

In this article, we categorize current inference-time techniques according to the following features:

1. **Computational and Memory Efficiency:** In general, even when utilizing the same algorithm, increased computational or memory resources during inference can result in higher-quality designs. For example, when using beam search with estimated value function, as the beam width increases, the performance increases while the computational time increases as illustrated in [Figure 3](#). Additionally, the ease of parallel computation is an important practical consideration.
2. **What Rewards We Want to Optimize:** In practice, choosing a good reward function that balances accuracy and computational efficiency is crucial. Besides, it is relevant to consider whether the attributes we aim to optimize (referred to as reward models in this draft) function as classifiers, as seen in the standard guidance literature, or as regressors, as is common in the literature on alignment. In this draft, the former task is often called *conditioning*, while the latter is called *alignment*.
3. **Differentiability of Reward Feedback:** In computer vision and NLP, many useful reward feedback is differentiable. However, in scientific domains such as molecular design, much of the useful reward feedback, such as physics-based simulations ([Salomon-Ferrer et al., 2013](#); [Chaudhury et al., 2010](#); [Trott and Olson, 2010](#)), is non-differentiable. Additionally, when utilizing learned reward models as feedback, they are often non-differentiable due to their reliance on non-differentiable features such as molecular fingerprints or biophysical descriptors ([Stanton and Jurs, 1990](#); [Yap, 2011](#); [Li et al., 2015](#)). This consideration is practically important, as it influences the choice of inference-time technique, as illustrated in [Figure 4](#).

Summary

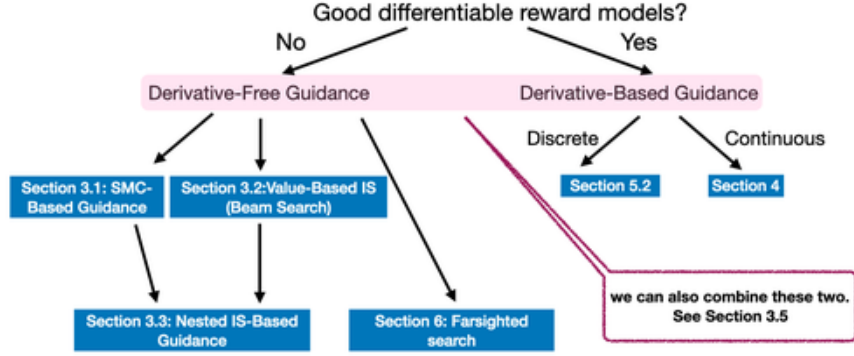


Figure 4: Roadmap of This Paper.

Considering these aspects, we provide a unified categorization of current inference-time techniques in diffusion models, while also highlighting novel perspectives. The key message of this tutorial is summarized as follows.

Key Message: A Unified Framework for Inference-Time Techniques in Diffusion Models

All methods introduced here (summarized in Figure 2) generally aim to approximately sample from specific target distributions. Denoting the reward function as $r : \mathcal{X} \rightarrow \mathbb{R}$ (e.g., classifiers or regressors) and $p^{\text{pre}}(\cdot)$ as the distribution induced by policies (i.e., denoising processes) from the pre-trained model, the target distribution is defined as

$$\underbrace{p^{\text{pre}}(\cdot)}_{\text{Pre-trained dist. (Naturalness)}} \times \underbrace{\exp(r(\cdot)/\alpha)}_{\text{Reward term (High functionality)}} / C \quad (:= \operatorname{argmax}_{p: \mathcal{X} \rightarrow \Delta(\mathcal{X})} \mathbb{E}_{x \sim p}[r(x)] - \alpha \text{KL}(p \| p^{\text{pre}})),$$

where C is the normalizing constant, and α is a hyperparameter. This distribution is desirable because the generated outputs exhibit both **naturalness** and **high functionality**.

To enable sampling from this distribution, by denoting pre-trained denoising process as $\{p_t^{\text{pre}}(\cdot | x_{t+1})\}_{t=T}^0$ (from $t = T$ to $t = 0$), all methods presented here (methods in Figure 2) employ the following distribution as the denoising process (i.e., optimal policies in RL) at each step during inference:

$$p_{t-1}^*(\cdot | x_t) := \underbrace{p_{t-1}^{\text{pre}}(\cdot | x_t)}_{\text{Pre-trained policies}} \times \underbrace{\exp(v_{t-1}(\cdot)/\alpha)}_{\text{Soft value functions}}, \quad (1)$$

where soft value functions act as look-ahead functions that predict the reward at the terminal state x_0 from intermediate state x_t (formalized later in Section 2). The primary distinction among inference-time algorithms lies in **how this approximation is achieved**, and the effectiveness of each method depends on the specific scenario.

Additionally, we explore more advanced aspects of inference-time methods in diffusion models, including their integration with fine-tuning, search algorithms, editing, and applications to masked

language models beyond diffusion frameworks. The remainder of this tutorial is organized as follows.

- **Section 2:** We start by outlining the foundational principles of inference-time techniques. Specifically, we introduce the soft optimal policy defined in (1), which represents the denoising process targeted during inference. All methods discussed in this tutorial aim to approximate this optimal policy.
- **Section 3:** We review inference-time techniques that do *not* require differentiable reward feedback, particularly useful in molecular design. These methods are roughly divided into two main categories: the SMC-based approach (Wu et al., 2024; Dou and Song, 2024; Cardoso et al., 2023; Phillips et al., 2024) and the value-based importance sampling approach (Li et al., 2024). Additionally, we explain how to integrate these two approaches.
- **Section 4, 5:** We review methods that require differentiable reward or value function models. This is useful when effective differentiable reward models can be constructed, such as for inpainting tasks in computer vision or motif scaffolding in protein design. We first discuss these methods for diffusion models in the continuous domain in Section 4, also known as classifier guidance (Dhariwal and Nichol, 2021; Song et al., 2021), with their formalization through Doob’s transform. Then, we provide an analogous explanation for discrete diffusion models in Section 5.
- **Section 6:** As mentioned in Section 3, beam search based on value functions is a natural solution for alignment tasks. A next natural step is to integrate more advanced search algorithms. We briefly discuss how search-based algorithms (e.g., MCTS) can be applied to diffusion models.
- **Section 7:** The inference-time techniques described in Sections Section 3 to Section 5 primarily focus on generating designs from fully noised states. However, in protein design, objectives often involve editing endogenous designs that meet stringent constraints. We examine how these objectives can be achieved by iteratively adapting the inference-time techniques presented in Sections Section 3 to Section 5 through sequential refinement.
- **Section 8:** We provide a concise review of inference-time techniques in language models, focusing on autoregressive models like GPT (Brown, 2020) and masked language models such as BERT (Kenton and Toutanova, 2019), and examine the similarities and differences between autoregressive models, masked language models, and diffusion models.
- **Section 9:** We describe how to apply inference-time techniques through distillation to fine-tune diffusion models. This is particularly important given that pure inference-time techniques can result in higher inference costs. We also establish connections between these methods and RL-based fine-tuning approaches.
- **Section 10:** We provide a brief overview of relevant algorithmic approaches in protein design, including walk-jump sampling (Frey et al., 2023) and hallucination methods (i.e., genetic algorithms, MCMC-based approaches) (Anishchenko et al., 2021; Jendrusch et al., 2021).

Application in Computational Protein Design

While our review primarily focuses on algorithms applicable to general domains, we provide a brief overview of how inference-time techniques can be applied to computational protein design to offer a concrete example. A key step in understanding how inference-time techniques operate is selecting pre-trained diffusion models and defining reward functions, as depicted in Figure 1. We discuss several options in the following sections. Code for this tutorial is available at <https://github.com/masauie/AlignInversePro>.

Pre-Trained Foundational Diffusion Models for Protein Sequences. Here, we briefly categorize foundational generative models capable of generating natural-like protein sequences. For additional references, see Winnifrieth et al. (2024), for example.

1. Purely Sequence-based Models: A common approach involves training discrete diffusion models exclusively on sequence datasets, without using structural datasets, as demonstrated in EvoDiff (Alamdari et al., 2023).

2. Structure-based Models: Another widely used approach involves explicit two-step procedures. In the first step, backbone structures are generated using diffusion models such as RFDiffusion (Watson et al., 2023) and Chroma (Ingraham et al., 2023). In the second step, protein sequences are generated conditioned on the backbone structure, a process often referred to as *inverse folding* such as ProteinMPNN (Dauparas et al., 2022).

3. Hybrid Models: Recent approaches leverage structural information in the above but do so seamlessly by jointly generating sequences and structures in each step, as proposed in Multiflow (Campbell et al., 2024), DPLM-2 (Wang et al., 2024), Protein Generator (Lisanza et al., 2023) and ESM3 (Hayes et al., 2024).

We note that the above foundational models are often introduced as conditional models. Typical conditions include secondary structures, motifs, domains, symmetry, etc.

Reward Models (Mapping Protein Sequences to Functionality). Here, we briefly outline practical approaches for constructing reward models. Common objectives we aim to optimize include binding affinity, stability, solubility, rigidity, etc. Ideally, reward models should be built using experimental data consisting of x (protein sequences) and y (target properties to be optimized, obtained from experimental assays). However, given the often limited size of such datasets, we frequently leverage features extracted from external “foundational” models trained on large datasets or incorporate external knowledge, such as physics-based insights. To construct these features, for example, we can utilize: (1) features derived from representation learning methods, such as

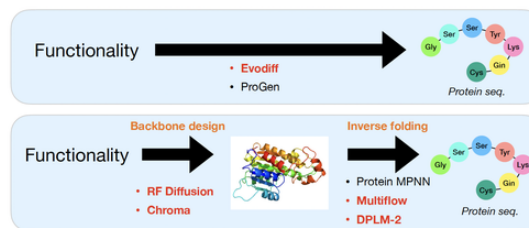


Figure 5: Typical foundational diffusion models for protein Sequences (especially, Red indicates diffusion models). The former approach relies solely on sequence data, while the latter explicitly generates the structure first, followed by the sequence. Notably, hybrid approaches that combine these methods have become increasingly popular in recent studies.

masked language models (e.g., ESM (Hayes et al., 2024)), (2) structural features based on predicted structures, and (3) biophysical features (e.g., ΔG computed through physics-based simulations).

In the absence of experimental data, it is practical to directly utilize outputs from “foundational” models or physics-based models as rewards. For instance, binding affinity can be assessed using outputs from AlphaFold3 (Abramson et al., 2024) or physics-based software such as Rosetta and AutoDock (Chaudhury et al., 2010; Trott and Olson, 2010).

Contents

1	Preliminaries	10
1.1	Diffusion Models	11
1.2	Objectives: Conditioning, Inverse Problems, Reward Maximization	13
1.2.1	Conditioning	14
1.2.2	Inverse Problems	14
1.2.3	Reward Maximization (i.e., Alignment)	15
2	Foundations of Inference-Time Controlled Generation	15
2.1	Soft Optimal Policies (Denoising Processes) in Diffusion Models	15
2.2	Approximating Soft Value Functions	18
2.2.1	Posterior Mean Approximation	18
2.2.2	Monte Carlo Regression	19
2.2.3	Soft Q-Learning	19
3	Derivative-Free Guidance	20
3.1	SMC-Based Guidance	20
3.2	Value-Based Importance Sampling	22
3.3	Nested-SMC-Based Guidance	23
3.4	Beam Search for Reward Maximization	24
3.5	Selecting Proposal Distributions	25
4	Derivative-Based Guidance in Continuous Diffusion Models	25
4.1	Intuitive Derivation of Classifier Guidance	26
4.2	Derivative-Free Guidance Versus Classifier Guidance	27
4.3	Continuous-Time Formalization via Doob transform	27
4.3.1	Preparation	27
4.3.2	Doob Transform	28
4.4	Guidance in Riemannian Diffusion Models	29
4.4.1	Primer: Riemannian Manifolds	29
4.4.2	Classifier Guidance in Riemannian Diffusion Models	30
5	Derivative-Based Guidance in Discrete Diffusion Models	31
5.1	Exact Sampling in Discrete Diffusion Models	31
5.2	Derivative-Based Guidance in Discrete Diffusion Models	34
5.3	Continuous-Time Formalization via Doob Transform	35
5.3.1	Preparation	35

5.3.2	Doob Transform in CTMC	36
6	Tree Search Algorithms for Alignment	37
6.1	Defining the Search Tree	37
6.2	How to Run Simulations from Leaf Nodes	37
7	Editing and Refinement with Diffusion Models	38
7.1	Iterative Refinement in Diffusion Models	39
7.2	Connection with Evolutionary Algorithms	39
8	Comparison with Inference-Time Techniques in Language Models	40
8.1	Inference-Time Alignment Technique in Autoregressive Models	40
8.1.1	Properties Leveraged in Diffusion Models	40
8.2	Inference-Time Alignment in Masked Language Models	41
8.2.1	Similarities and Differences Compared to Masked Diffusion Models	41
8.2.2	Adaptation of Alignment Methods	42
9	Combining Fine-Tuning with Inference-Time Techniques	43
9.1	Comparison with Standard Post-Training Methods	44
9.1.1	Classifier-Free Fine-Tuning	44
9.1.2	RL-Based Fine-Tuning	45
9.2	Policy Distillation	45
9.2.1	Choice of Roll-In Distributions	46
9.2.2	Choice of Divergence	47
9.3	Relation to RL-Based Fine-Tuning	48
9.3.1	Value-Weighted MLE (Reward-Weighted MLE)	48
9.3.2	Path Consistency Learning (loss used in Gflownets)	48
9.3.3	PPO and Direct Backpropagation	49
9.4	Differences between Policy Distillation and RL-Based Fine-Tuning	49
9.5	Further Extensions with “Distillation”	50
10	More Related Works	51
10.1	Walk-Jump Sampling for Protein Design	51
10.2	Hallucination Approaches for Protein Design	51
10.3	Inference-Time Techniques for Inpainting and Linear Inverse Problems.	52
10.4	Speculative Decoding.	52

1 Preliminaries

In this section, we begin by discussing the fundamentals of diffusion models. We then formalize our objectives, such as conditioning or alignment (i.e., reward maximization), during inference without fine-tuning. Finally, we introduce several post-training approaches (RL-based fine-tuning and classifier-free guidance) and compare them with purely inference-time techniques.

1.1 Diffusion Models

In diffusion models (Sohl-Dickstein et al., 2015; Ho et al., 2020; Song et al., 2020), the goal is to learn a sampler $p^{\text{pre}}(\cdot) \in \Delta(\mathcal{X})$ for a given design space \mathcal{X} using datasets. For instance, in protein conformation generation, \mathcal{X} may be a Euclidean space if 3D coordinates are used as inputs or a Riemannian manifold if torsion angles are employed, and in protein inverse folding, \mathcal{X} corresponds to a discrete space.

Our objective in training diffusion models is to learn a sequential mapping (i.e., a denoising process) that transitions from a noise distribution to the true data distribution. The training procedure is summarized as follows: Initially, a forward *noising* process $q_t : \mathcal{X} \rightarrow \Delta(\mathcal{X})$ is pre-defined, spanning from $t = 0$ to $t = T$. Here, we often refer to such a noising process as a *policy*, following the terminology of RL in our tutorial.

Then, our goal is to learn a reverse *denoising* process p_t , where each p_t is $\mathcal{X} \rightarrow \Delta(\mathcal{X})$, ensuring that the distributions induced by both the forward and backward processes are marginally equivalent. To achieve this, the backward processes are parameterized by $\theta \in \mathbb{R}^d$ through neural networks, and the following loss function is optimized:

$$\mathbb{E}_{x_1, \dots, x_T \sim q(\cdot | x_0)} \left[-\log p_0(x_0 | x_1) + \sum_{t=1}^{T-1} \text{KL}(q_t(\cdot | x_{t-1}, x_0) \| p_t(\cdot | x_{t+1}; \theta)) + \text{KL}(q_T(\cdot) \| p_T(\cdot)) \right],$$

where the expectation is taken with respect to the distribution induced by the forward process. This loss function represents the variational lower bound of the negative log-likelihood $-\log p(x_0)$, commonly known as the ELBO.

The remaining question is how to define the noising and denoising processes. Below are examples of concrete parameterizations for these processes in Euclidean space and discrete space.

Example 1 (Euclidean space). *When \mathcal{X} is a Euclidean space, we typically use the Gaussian distribution $q_t(\cdot | x_t) = \mathcal{N}(\sqrt{\alpha_t}x_t, (1 - \alpha_t)\mathbf{I})$ as the forward noising process where \mathbf{I} is an identity matrix, where $\alpha_t \in \mathbb{R}$ denote a noise schedule. Then, the backward process is parameterized as*

$$\mathcal{N}\left(\frac{\sqrt{\alpha_t}(1 - \bar{\alpha}_{t-1})x_t + \sqrt{\bar{\alpha}_{t-1}}(1 - \alpha_t)\hat{x}_0(x_t; \theta)}{1 - \bar{\alpha}_t}, \sigma_t^2 \mathbf{I}\right), \quad \sigma_t^2 = \frac{(1 - \alpha_t)(1 - \bar{\alpha}_{t-1})}{1 - \bar{\alpha}_t}, \quad (2)$$

where $\bar{\alpha}_t = \prod_{i=1}^t \alpha_i$. The loss function for θ is

$$\sum_t \mathbb{E}_{x_t \sim q_t(\cdot | x_0)} [w(t) \|\hat{x}_0(x_t; \theta) - x_0\|_2^2]$$

where w is a weighting function: $w : [0, T] \rightarrow \mathbb{R}$ and $q_t(\cdot | x_0)$ is a distribution induced by forward policies from 0 to t . A typical choice of $w(t)$ is $\lambda(t-1) - \lambda(t)$ where $\lambda(t) = \bar{\alpha}_t / (1 - \bar{\alpha}_t)$. Here, $\hat{x}_0(x_t; \theta)$ is a neural network that predicts x_0 from x_t (i.e., $\mathbb{E}_{x_0 \sim q(\cdot | x_t)} [x_0 | x_t]$).

Remark 1 (Different parameterization). *In the above diffusion models for continuous domains, we also note that there are two additional ways of parameterization. For further details, see Luo (2022). The first parameterization involves predicting the noise ϵ_0 rather than x_0 , recalling that*

$x_t = \sqrt{\alpha_t}x_0 + \sqrt{1 - \alpha_t}\epsilon_0$, $\epsilon_0 \sim \mathcal{N}(0, \mathbf{I})$. In this case, using the relation $x_0 = (x_t - \sqrt{1 - \alpha_t}\epsilon_0)/\sqrt{\alpha_t}$, the mean in the backward denoising process (2) is parameterized as

$$\frac{1}{\sqrt{\alpha_t}} \left(x_t - \frac{1 - \alpha_t}{\sqrt{1 - \bar{\alpha}_t}} \hat{\epsilon}_0(x_t; \theta) \right).$$

Another parameterization is the score parameterization, which aims to estimate $\nabla_{x_t} \log q_t(x_t)$ where q_t is a marginal distribution at time t induced by forward noising processes. In this case, the mean in the backward denoising process (2) is

$$\frac{1}{\sqrt{\alpha_t}} \left(x_t + (1 - \alpha_t) \widehat{\nabla_{x_t} \log p(x_t; \theta)} \right).$$

In particular, when $\alpha_t = 1 - (\delta t)$ for small δt , ignoring second-order terms $O((\delta t)^2)$, the above expression simplifies to:

$$x_t + (\delta t) \left\{ 0.5x_t + \widehat{\nabla_{x_t} \log p(x_t; \theta)} \right\}, \quad \sigma_t^2 = (\delta t). \quad (3)$$

Example 2 (Discrete space (masked diffusion models)). Here, we explain masked diffusion models (Sahoo et al., 2024; Shi et al., 2024), inspired by seminal works on discrete diffusion models (e.g., Austin et al. (2021); Campbell et al. (2022); Lou et al. (2023)).

Let \mathcal{X} be a space of one-hot column vectors $\{x \in \{0, 1\}^K : \sum_{i=1}^K x_i = 1\}$, and $\text{Cat}(\pi)$ be the categorical distribution over K classes with probabilities given by $\pi \in \Delta^K$ where Δ^K denotes the K -simplex. A typical choice of the forward noising process is $q(x_{t+1} | x_t) = \text{Cat}(\alpha_t x_t + (1 - \alpha_t) \mathbf{m})$ where $\mathbf{m} = \underbrace{[0, \dots, 0]}_{K-1}, \text{Mask}$. Then, the backward process is

parameterized as

$$x_{t-1} = \begin{cases} \delta(\cdot = x_t) & \text{if } x_t \neq \mathbf{m} \\ \text{Cat} \left(\frac{(1 - \bar{\alpha}_{t-1}) \mathbf{m} + (\bar{\alpha}_{t-1} - \bar{\alpha}_t) \hat{x}_0(x_t; \theta)}{1 - \bar{\alpha}_t} \right) & \text{if } x_t = \mathbf{m}, \end{cases}$$

where $\bar{\alpha}_t = \prod_{i=1}^t \alpha_i$. The loss function for θ is

$$\sum_t \mathbb{E}_{x_t \sim q_t(\cdot | x_0)} [w(t) \mathbf{I}(x_t = \mathbf{m}) \langle x_0, \log \hat{x}_0(x_t; \theta) \rangle] \quad (4)$$

where w is a weight function. A typical choice of $w(t)$ is $\lambda(t - 1) - \lambda(t)$ where $\lambda(t) = \bar{\alpha}_t / (1 - \bar{\alpha}_t)$.

Here, $\hat{x}_0(x_t; \theta)$ is a neural network that predicts x_0 from x_t (when x_t is masked). Note that the above loss function is similar to the one used in BERT (Devlin, 2018). Compared to BERT, masked diffusion models are more hierarchical, with a greater variety of masking modes. Given the success of BERT-type algorithms for biological sequences, such as ESM (Hayes et al., 2024) for protein, DNA BERT (Ji et al., 2021), RNA BERT (Akiyama and Sakakibara, 2022), CodonBERT (Ren et al., 2024), the application of discrete diffusion models to biological sequences is considered as a natural extension.

Remark 2. Multiple tokens In the above, we focused on the case of a single token. When considering a sequence of L tokens ($x^{1:L}$), we employ noising/denoising processes defined as $p_{t-1}(x_{t-1}^{1:L}|x_t^{1:L}) = \prod_{l=1}^L p_{t-1}(x_{t-1}^l|x_t^{1:L})$, which is independent across tokens. This independence is crucial for mitigating the curse of token length, i.e., avoiding the need to directly model the entire space with a cardinality of $O(K^L)$. This aspect also plays a significant role in the inference-time techniques discussed later in [Section 5.1](#), as also highlighted in [Nisonoff et al. \(2024\)](#).

After learning the backward process as in the above examples, we can sample from a distribution that emulates training data distribution (i.e., $p^{\text{pre}}(x)$) by sequentially sampling $\{p_t\}_{t=T}^0$ from $t = T$ to $t = 0$. In this draft, given a pre-trained model $\{p_t^{\text{pre}}\}_{t=T}^0$, we denote the induced distribution by $p^{\text{pre}}(x)$, i.e.,

$$p^{\text{pre}}(x_0) = \int \left\{ \prod_{t=T+1}^1 p_{t-1}^{\text{pre}}(x_{t-1}|x_t) \right\} dx_{1:T}.$$

Here, with slight abuse of notation, we denote $p_T^{\text{pre}}(\cdot | \cdot)$ by $p_T^{\text{pre}}(\cdot)$.

Conditional Generative Models. Note that while the following discussion assumes pre-trained models are unconditional generative models, it can be easily extended to cases where pre-trained models are conditional generative models, $p(x | c) : \mathcal{C} \rightarrow \Delta(\mathcal{X})$. For instance, in protein conformation generation, c represents a 1D amino acid sequence, and x is the corresponding protein conformation. In protein inverse folding, c typically refers to a backbone structure, and x is a 1D amino acid sequence. The training process for conditional diffusion models is nearly identical to that of unconditional models, with the only difference being the need to augment the input of the denoising process with the additional space \mathcal{C} . In this process, we typically introduce an additional “unconditional class”, as implemented in classifier-free guidance ([Ho et al., 2020](#)).

Notation. The notation δ_a denotes a Dirac delta distribution centered at a . The notation \propto indicates that the distribution is equal up to a normalizing constant. With slight abuse of notation, we often denote $p_T(\cdot|\cdot)$ by $p_T(\cdot)$. The notation $\text{Cat}([w_1, \dots, w_M])$ means a categorical distribution with probability $[w_1, \dots, w_M]$.

1.2 Objectives: Conditioning, Inverse Problems, Reward Maximization

In this review, we consider a scenario where a pre-trained diffusion model has been trained on a large dataset. For example, this could be an unconditional generative model that captures the natural-like protein space. Then, at inference time (during sampling), we aim to guide the generation process to achieve a specific objective. Generally, we seek to optimize a reward function $r : \mathcal{X} \rightarrow \mathbb{R}$ that characterizes this objective, such as the binding affinity of proteins. Later, we will discuss how to define such rewards in more detail. Mathematically, the goal above is formalized as follows.

Overall General Objectives

We aim to generate designs that achieve high rewards while preserving the naturalness of the samples. More specifically, our goal is to sample from the distribution:

$$p^{(\alpha)}(\cdot) := \frac{\exp(r(\cdot)/\alpha)p^{\text{pre}}(\cdot)}{\int \exp(r(x)/\alpha)p^{\text{pre}}(x)dx} = \underset{p \in [\Delta(\mathcal{X})]}{\operatorname{argmax}} \underbrace{\mathbb{E}_{x \sim p(\cdot)}[r(x)]}_{\text{Term (a): Reward}} - \alpha \underbrace{\text{KL}(p(\cdot) \| p^{\text{pre}}(\cdot))}_{\text{Term (b): Naturalness}}. \quad (5)$$

Term (a) is introduced to optimize the reward function, while term (b) ensures the naturalness of the generated samples. For instance, in protein design, this formulation aligns with the objective of generating natural-like proteins that exhibit high functionality.

In the following, we provide detailed examples of reward functions, categorized into three primary scenarios: (a) conditioning problems, (b) inverse problems, and (c) alignment problems. To summarize, in conditioning, rewards are typically classifiers; in inverse problems, rewards are (known) likelihoods; and in alignment problems, rewards are regressors. However, it is important to note that these scenarios are often treated in a mixed manner in the literature.

1.2.1 Conditioning

In scenarios where we aim to sample from conditional distributions $p(x | y) \in [\mathcal{Y} \rightarrow \Delta(\mathcal{X})]$, a natural choice for the reward function r is the log-likelihood $\log p(y | x)$, defined by a classifier $p(y | x)$. This classifier is often not predefined and must be learned from datasets consisting of paired samples (x, y) . For example, in protein design, classifiers that categorize protein functions/families (such as enzymes, transport proteins, and receptors) serve as effective reward functions. In particular, setting $\alpha = 1$ enables the generation of samples directly from $p(x | y)$, as demonstrated by the following derivation:

$$p^{(1)}(x|y) \propto \exp(\log p(y|x))p^{\text{pre}}(x) = p(y|x)p^{\text{pre}}(x) \underset{\text{Bayes theorem}}{\propto} p(x|y).$$

1.2.2 Inverse Problems

A closely related challenge to the conditioning problem is the inverse problem, where the objective is to sample from $p(x | y) \in [\mathcal{Y} \rightarrow \Delta(\mathcal{X})]$. In inverse problems, we typically assume a known observation model:

$$y = \mathcal{A}(x) + n,$$

where $\mathcal{A} : \mathcal{X} \rightarrow \mathcal{Y}$ represents the measurement operator, n denotes measurement noise, and \mathcal{Y} is a possibly high-dimensional continuous space. When n follows a Gaussian distribution, the log-likelihood can be expressed explicitly, resulting in the following reward function: $\|y - \mathcal{A}(x)\|_2^2$.

This type of problem frequently arises in computer vision applications, where constructing a conditional model $p(x | y)$ without classifier-free guidance is particularly challenging due to the high dimensionality of y . A canonical example of an inverse problem is image inpainting, where the objective is to restore missing or corrupted regions of an image in a visually coherent manner. In the field of protein design, analogous tasks include motif scaffolding, where the goal is to generate

a scaffold (the complete stable backbone structure) conditioned on the motif (functionally critical structural or sequence elements).

1.2.3 Reward Maximization (i.e., Alignment)

The primary objective in alignment problems is to optimize specific downstream reward functions, often represented by regressors. This task is critical in natural language processing (NLP) and computer vision (CV), commonly referred to as alignment. In protein design, it typically involves maximizing metrics such as binding affinity, immunogenicity, designability, self-consistency, and stability (Hayes et al., 2024; Wang et al., 2024; Widatalla et al., 2024; Ingraham et al., 2023; Hie et al., 2022).

Below, we outline several key considerations:

- **Known or Unknown Rewards:** In many cases, reward functions can be predefined (i.e., not requiring learning) when optimizing metrics such as docking scores and stability from physics-based simulations or properties like SA, QED, and logP calculated using RDKit in molecular design. However, in many other scenarios, these rewards must be learned from experimental data.
- **Quality vs. Computational Efficiency:** Even when rewards are directly obtained from physics-based simulations, high-resolution simulations can be computationally prohibitive. For instance, Glide (Halgren et al., 2004) offers high accuracy, while AutoDock Vina (Trott and Olson, 2010) is significantly faster but sacrifices accuracy. When selecting specific objectives, balancing the trade-off between computational efficiency and accuracy is a crucial practical challenge.
- **Multi-Objectiveness:** In molecular design, it is often necessary to optimize multiple objective functions simultaneously. For example, in small molecule generation, the goal is to control properties such as affinity, specificity, designability, lipophilicity, and toxicity. However, since these reward functions often conflict, achieving optimal trade-offs poses a significant challenge.

2 Foundations of Inference-Time Controlled Generation

In this section, we establish the foundation of inference-time techniques in diffusion models. Specifically, we describe the form of the optimal policy (i.e., denoising process) for the objective introduced in Section 1.2, which involves guiding natural-like designs with high functionality. All the methods presented in the following sections, from Section 3 to Section 5, aim to approximate this policy.

2.1 Soft Optimal Policies (Denoising Processes) in Diffusion Models

We introduce several key concepts essential for understanding our target policies (i.e., target denoising processes) for inference-time techniques that are detailed in the following section. These concepts are well established through the lens of RL, recognizing that diffusion models can be framed with MDPs. For further details, refer to Uehara et al. (2024, Section 3). A summary is provided below.



Figure 6: Formulating diffusion models using MDPs.

Soft Value Function. For $t \in [T + 1, \dots, 1]$, we define the *soft value function* as:

$$v_{t-1}(\cdot) := \alpha \log \mathbb{E}_{x_0 \sim p^{\text{pre}}(x_0|x_{t-1})} \left[\exp \left(\frac{r(x_0)}{\alpha} \right) | x_{t-1} = \cdot \right], \quad (6)$$

where $\mathbb{E}_{x_0 \sim p^{\text{pre}}(x_0|x_{t-1})}[\cdot]$ is induced by pre-trained policies $\{p_t^{\text{pre}}(\cdot|x_{t+1})\}_{t=T}^0$. Since this plays a key role in our tutorial, we highlight it as follows:

Soft Value Function

This soft value function captures the expected future reward at $t = 0$ from the intermediate state at $t - 1$. Intuitively, it serves as a look-ahead function that predicts future rewards $r(x_0)$ based on the intermediate state x_{t-1} . It enables us to guide an inference procedure efficiently from $t = 0$ to $t = T$, as we will see shortly.

To further illustrate, consider a scenario where r is a classifier $r(\cdot) = \log p(y|\cdot)$ for class y and $\alpha = 1$. In this case, the above expression simplifies to:

$$v_{t-1}(\cdot) = \log \mathbb{E}_{x_0 \sim p^{\text{pre}}(x_0|x_{t-1})} [p(y|x_0) | x_{t-1} = \cdot],$$

which aligns with the formulation used in classifier guidance (Dhariwal and Nichol, 2021; Song et al., 2021).

Soft-Bellman Equation. Soft-Bellman equations (e.g., Haarnoja et al. (2017); Geist et al. (2019)) characterize value functions recursively as follows:

$$\int p_{t-1}^{\text{pre}}(x|x_t) \exp(v_{t-1}(x)/\alpha) dx = \exp(v_t(x_t)/\alpha). \quad (7)$$

By iterating the above equation, we can easily derive (6) as follows:

$$\begin{aligned} \exp \left(\frac{v_t(x_t)}{\alpha} \right) &= \mathbb{E}_{p^{\text{pre}}} \left[\exp \left(\frac{v_{t-1}(x_{t-1})}{\alpha} \right) | x_t \right] = \mathbb{E}_{p^{\text{pre}}} \left[\exp \left(\frac{v_{t-2}(x_{t-2})}{\alpha} \right) | x_t \right] = \dots \\ &= \mathbb{E}_{p^{\text{pre}}} \left[\exp \left(\frac{r(x_0)}{\alpha} \right) | x_t \right]. \end{aligned}$$

Soft Optimal Policy. We define the *soft optimal policy* $p_{t-1}^* : \mathcal{X} \rightarrow \Delta(\mathcal{X})$ as a weighted pre-trained policy with value functions $v_{t-1} : \mathcal{X} \rightarrow \mathbb{R}$:

$$p_{t-1}^*(\cdot|x_t) = \frac{p_{t-1}^{\text{pre}}(\cdot|x_t) \exp(v_{t-1}(\cdot)/\alpha)}{\int_{x \in \mathcal{X}} p_{t-1}^{\text{pre}}(x|x_t) \exp(v_{t-1}(x)/\alpha) dx}. \quad (8)$$

Intuitively, this policy retains the characteristics of the pre-trained policy while guiding generation toward optimizing reward functions through soft value functions. Using the soft-Bellman equation (7) and substituting the denominator in (8), the above optimal policy simplifies to

$$p_{t-1}^*(\cdot|x_t) = \frac{p_{t-1}^{\text{pre}}(\cdot|x_t) \exp(v_{t-1}(\cdot)/\alpha)}{\exp(v_t(x_t)/\alpha)}.$$

The term “optimal” reflects that this policy maximizes the following entropy-regularized objective:

$$\operatorname{argmax}_{\{p_t: \mathcal{X} \rightarrow \Delta(\mathcal{X})\}_{t=T}^0} \mathbb{E}_{\{p_t\}_{t=T}^0} \left[r(x_0) - \alpha \sum_{t=T}^0 \text{KL}(p_{t-1}(\cdot|x_t) \| p_{t-1}^{\text{pre}}(\cdot|x_t)) \right],$$

which is a standard objective in RL-based fine-tuning for diffusion models (Fan et al., 2023; Uehara et al., 2024).

With this setup, we present the following key theorem:

Theorem 1 (From Theorem 1 in Uehara et al. (2024)). *The distribution induced by $\{p_t^*(\cdot|x_{t+1})\}_{t=T}^0$ (i.e., $\int \{\prod_{t=T+1}^1 p_{t-1}^*(x_{t-1}|x_t)\} dx_{1:T}$) is the target distribution $p^{(\alpha)}(\cdot)$ in (5), i.e.,*

$$\frac{\exp(r(\cdot)/\alpha) p^{\text{pre}}(\cdot)}{\int_{x \in \mathcal{X}} \exp(r(x)/\alpha) p^{\text{pre}}(x) dx}.$$

Thus, by sequentially sampling from soft optimal policies during inference, we can generate natural-like designs with high functionality. However, this approach presents practical challenges due to two key factors:

1. The absence of an exact value function $v_t(\cdot)$
2. The large action space \mathcal{X} , making it challenging to compute the normalizing constant in the denominator (i.e., $\int_{x \in \mathcal{X}} \exp(r(x)/\alpha) p^{\text{pre}}(x) dx$) or evaluate value functions in the numerator within a reasonable computational time.

In the following section, we first review methods that address the first challenge of value function approximation in Section 2.2, followed by approaches that attempt to address the second challenge using these approximated value functions in Section 3-Section 5. The key message is as follows.

Takeaways

Each guidance method discussed in this tutorial aims to approximate the soft-optimal policy through different approaches. The method in Section 3 seeks to achieve this approximation in a derivative-free manner, while the methods in Section 4 and 5 leverage the gradient of value functions to approximate the policy.

Before addressing solutions to the first challenge, we highlight several additional points related to Theorem 1.

- **Extension from Discrete-Time to Continuous-Time Formulation:** Although [Theorem 1](#) is formulated for discrete-time diffusion models, it has been extended to continuous-time diffusion models in later work. See [Uehara et al. \(2024, Theorem 1\)](#) for continuous space diffusion models and [Wang et al. \(2024, Theorem 1\)](#) for discrete space diffusion models.
- **RL-Based Fine-Tuning:** In RL-based fine-tuning, this framework is implicitly employed as the target policy. However, practical implementations differ due to various associated errors (e.g., optimization or function approximation errors), and value functions are typically not directly employed in RL-based fine-tuning.
- **Avoiding Curse of Token Length in Discrete Diffusion Models:** In discrete diffusion models ([Example 2](#)), the space \mathcal{X} appears to be K^L , where K is the vocabulary size and L is the token length. However, the effective action space is actually KL , enabling exact sampling from optimal policies (with approximated value functions) when L and K are relatively small. We will discuss this aspect in more detail in [Section 5.1](#).
- **For Pre-Defined MDPs:** Our results can be readily extended to scenarios where MDPs are pre-defined, particularly in synthesizable molecular generation ([Cretu et al., 2024](#); [Seo et al., 2024](#)). This setting has been widely explored in the literature on GFlowNets ([Bengio et al., 2023](#)).
- **Relation with Other Works:** Similar (and essentially equivalent) results to [Theorem 1](#) have been known in various fields, including soft RL ([Haarnoja et al., 2017](#); [Levine, 2018](#)), language models ([Mudgal et al., 2023](#); [Han et al., 2024](#)). In addition, in the computational statistics literature, soft value functions are referred to as twisting potentials, while soft optimal policies are known as optimally twisted policies ([Doucet et al., 2009](#); [Naesseth et al., 2019](#); [Heng et al., 2020](#)).

2.2 Approximating Soft Value Functions

We present several representative methods for approximating value functions, each of which can be integrated into inference-time techniques. They are used for the inference-time technique discussed in subsequent sections, recalling that the inference-time technique aims to approximate soft-optimal policies, which are expressed as the product of value functions and pre-trained policies.

2.2.1 Posterior Mean Approximation

The most straightforward approach is to use the following approximation:

$$\mathbb{E}_{x_0 \sim p^{\text{pre}}(x_t)}[r(x_0)|x_t] = \int r(x_0)p^{\text{pre}}(x_0|x_t)dx_0 \approx r(\mathbb{E}_{x_0 \sim p^{\text{pre}}(x_t)}[x_0|x_t]).$$

In pre-trained models, we have a decoder from x_t to x_0 , denoted by $\hat{x}_0(x_t)$ in [Example 1](#) and [2](#). Thus, a natural approach is to use $r(\hat{x}_0(x_t))$. The whole algorithm is summarized in [Algorithm 1](#). This approximation has been applied for conditioning where the reward functions are classifiers, such as in DPS ([Chung et al., 2022](#)), universal guidance ([Bansal et al., 2023](#)), and reconstruction guidance ([Ho et al., 2022](#)).

Algorithm 1 Value Function Estimation using Posterior Mean Approximation

Require: Pre-trained diffusion models, reward $r : \mathcal{X} \rightarrow \mathbb{R}$

Set $\hat{v}^\diamond(\cdot, t) := r(\hat{x}_0(x_t = \cdot))$

Output: \hat{v}^\diamond

2.2.2 Monte Carlo Regression

Another natural approach is to train a value function regressor. From the definition (6) of soft value functions, we can show:

$$\exp(v(\cdot)/\alpha) = \operatorname{argmin}_{f:\mathcal{X}\rightarrow\mathbb{R}} \mathbb{E}_{x_0\sim p^{\text{pre}}(x_t), x_t\sim u_t} [\{\exp(r(x_0)/\alpha) - f(x_t)\}^2],$$

where $u_t \in \Delta(\mathcal{X})$ represents a roll-in distribution. By replacing this approximation with an empirical objective and applying function approximation, the complete algorithm is summarized in [Algorithm 2](#) when we use distributions induced by pre-trained models as roll-in distributions.

Algorithm 2 Value Function Estimation using Monte Carlo Regression

1: **Require:** Pre-trained diffusion models $\{p_t^{\text{pre}}\}_{t=T}^0$, reward $r : \mathcal{X} \rightarrow \mathbb{R}$, function class $\Phi : \mathcal{X} \times [0, T] \rightarrow \mathbb{R}$.

2: Collect datasets $\{x_T^{(s)}, \dots, x_0^{(s)}\}_{s=1}^S$ by rolling-out $\{p_t^{\text{pre}}\}_{t=T}^0$ from $t = T$ to $t = 0$.

3:

$$\hat{f} = \operatorname{argmin}_{f \in \Phi} \sum_{t=T}^0 \sum_{s=1}^S \left\{ \exp\left(\frac{r(x_0^{(s)})}{\alpha}\right) - \exp\left(\frac{f(x_t^{(s)}, t)}{\alpha}\right) \right\}^2.$$

4: **Output:** $\hat{f}(\cdot)$

2.2.3 Soft Q-Learning

Another natural approach is to use soft Q-learning ([Haarnoja et al., 2017](#); [Levine, 2018](#)). Recall the soft-Bellman equations (7), we have:

$$\exp\left(\frac{v_t(\cdot)}{\alpha}\right) = \operatorname{argmin}_{f:\mathcal{X}\rightarrow\mathbb{R}} \mathbb{E}_{x_t\sim u_t} \left[\left\{ \exp\left(\frac{v_{t-1}(x_{t-1})}{\alpha}\right) - f(x_t) \right\}^2 \right],$$

where $u_t \in \Delta(\mathcal{X})$ is a roll-in distribution. Although the right-hand side is not directly accessible, we can estimate the value functions by recursively applying regression, a procedure known as Fitted Q-iteration (FQI) in RL ([Ernst et al., 2005](#); [Mnih et al., 2015](#)). The complete algorithm is summarized in [Algorithm 3](#).

Algorithm 3 Value Function Estimation using Soft Q-learning

- 1: **Require:** Pre-trained diffusion models $\{p_t^{\text{pre}}\}_{t=T}^0$, value function class $\Phi : \mathcal{X} \times [0, T] \rightarrow \mathbb{R}$
- 2: Collect datasets $\{x_T^{(s)}, \dots, x_0^{(s)}\}_{s=1}^S$ by rolling-out $\{p_t^{\text{pre}}\}_{t=T}^0$ from $t = T$ to $t = 0$.
- 3: **for** $j \in [0, \dots, J]$ **do**
- 4: Run regression:

$$\hat{f}^j \leftarrow \operatorname{argmin}_{f \in \Phi} \sum_{t=T}^0 \sum_{s=1}^S \left\{ \exp \left(\frac{f(x_t^{(s)})}{\alpha} \right) - \exp \left(\frac{\hat{f}^{j-1}(x_{t-1}^{(s)})}{\alpha} \right) \right\}^2.$$

- 5: **end for**
 - 6: **Output:** $\alpha \log \hat{f}^J$
-

3 Derivative-Free Guidance

We begin by outlining two primary derivative-free approaches that do not rely on differentiable models. As discussed in the introduction, constructing differentiable models in molecular design can be challenging due to the non-differentiable nature of reward feedback for the following reasons.

Scenarios where Non-Differentiable Reward Feedback is Beneficial

- Reward feedback is often provided through black-box physics-based simulations (e.g., docking simulations).
- Non-differentiable features (e.g., molecular descriptors) may be required to build reward models.
- Reward models may involve non-differentiable architectures, such as specified graph neural networks or XGBoost.

Therefore, these derivative-free methods are particularly useful in such scenarios. In this section, we first introduce sequential Monte Carlo (SMC)-based guidance, followed by value-based importance sampling approach.

3.1 SMC-Based Guidance

We first provide an intuitive explanation of SMC-based guidance proposed in [Wu et al. \(2024\)](#); [Dou and Song \(2024\)](#); [Cardoso et al. \(2023\)](#); [Phillips et al. \(2024\)](#), which combine SMC (a.k.a. particle filter) ([Gordon et al., 1993](#); [Kitagawa, 1993](#); [Del Moral et al., 2006](#)) with diffusion models. While there are several variants, we focus here on the simplest version. Since SMC-based guidance is an iterative method, let us consider the process at t . At this stage, we assume there are N samples (particles), $\{x_t^{[i]}\}_{i=1}^N$, each with uniform weights: $1/N \sum_{i=1}^N \delta_{x_t^{[i]}}$. Given this distribution, our goal is to sample from the optimal policy $p_{t-1}^*(\cdot | \cdot)$.

For this purpose, using a proposal distribution $q_{t-1}(\cdot | x_t^{[i]}) : \mathcal{X} \rightarrow \Delta(\mathcal{X})$, such as policies from pre-trained models (we will discuss this choice further in [Section 3.5](#)), we generate new samples $\{\bar{x}_{t-1}^{[i]}\}$. Ideally, we aim to sample from the optimal policy in (6). To approximate this, based on

importance sampling, we consider the following weighted empirical distribution:

$$\sum_{i=1}^N \frac{w_{t-1}^{[i]}}{\sum_{j=1}^N w_{t-1}^{[j]}} \delta_{\bar{x}_{t-1}^{[i]}}, \quad w_{t-1}^{[i]} = \frac{p_{t-1}^*(\bar{x}_{t-1}^{[i]}|x_t^{[i]})}{q_{t-1}(\bar{x}_{t-1}^{[i]}|x_t^{[i]})} = \frac{p_{t-1}^{\text{pre}}(\bar{x}_{t-1}^{[i]}|x_t^{[i]}) \exp(v(\bar{x}_{t-1}^{[i]})/\alpha)}{q_{t-1}(\bar{x}_{t-1}^{[i]}|x_t^{[i]}) \exp(v(x_t^{[i]})/\alpha)}.$$

However, as the weights become increasingly non-uniform, the approximation quality deteriorates. To mitigate this, SMC performs resampling with replacement, generating an equally weighted Dirac delta distribution:

$$\frac{1}{N} \sum_{i=1}^N \delta_{x_{t-1}^{[i]}}, \quad x_{t-1}^{[i]} := \bar{x}_{t-1}^{[\zeta_i]}, \quad \zeta_i \sim \text{Cat} \left[\left\{ \frac{w_{t-1}^{[i]}}{\sum_{j=1}^N w_{t-1}^{[j]}} \right\}_{i=1}^N \right]. \quad (9)$$

The complete algorithm is summarized in [Algorithm 4](#). Note that to maintain computational efficiency, the resampling step (9) is executed when the effective sample size, which indicates the degree of weight uniformity, falls below a predefined threshold.

Algorithm 4 SMC-Based Guidance (e.g., [Wu et al. \(2024\)](#); [Dou and Song \(2024\)](#); [Cardoso et al. \(2023\)](#); [Phillips et al. \(2024\)](#))

- 1: **Require:** Estimated (potentially **non-differentiable**) value functions $\{\hat{v}_t(x)\}_{t=T}^0$ ([Section 2.2](#)), pre-trained diffusion models $\{p_t^{\text{pre}}\}_{t=T}^0$, proposal policies $\{q_t\}_{t=T}^0$, hyperparameter $\alpha \in \mathbb{R}$, Batch size N
- 2: **for** $t \in [T + 1, \dots, 1]$ **do**
- 3: **Importance sampling step:** Generate $i \in [1, \dots, N]$; $x_{t-1}^{[i]} \sim q_{t-1}(\cdot|x_t^{[i]})$
- 4: Update weights:

$$w^{[i]} \leftarrow \frac{p_{t-1}^{\text{pre}}(x_{t-1}^{[i]}|x_t^{[i]}) \exp(\hat{v}_{t-1}(x_{t-1}^{[i]})/\alpha)}{q_{t-1}(x_{t-1}^{[i]}|x_t^{[i]}) \exp(\hat{v}_t(x_t^{[i]})/\alpha)} w^{[i]}.$$

- 5: **Resampling step:** Calculate the effective sample size $\frac{\{\sum_i w^{[i]}\}^2}{\sum \{w^{[i]}\}^2}$. If it falls below a certain threshold, resample by selecting new indices with replacement:

$$\{x_{t-1}^{[i]}\}_{i=1}^N \leftarrow \{x_{t-1}^{\zeta_{i-1}}\}_{i=1}^N, \quad \{\zeta_{i-1}\}_{i=1}^N \sim \text{Cat} \left(\left\{ \frac{w_{t-1}^{[i]}}{\sum_{j=1}^N w_{t-1}^{[j]}} \right\}_{i=1}^N \right).$$

- 6: **end for**
 - 7: **Output:** $\{x_0^{[i]}\}_{i=1}^N$
-

Finally, we highlight several additional considerations:

- **Potential Lack of Diversity:** In practice, SMC-generated samples may suffer from sample collapse (i.e., generating the same sample in one batch) for the purpose of reward maximization. This occurs because, as $\alpha \rightarrow 0$, the effective sample size approaches 1. Another challenge with SMC-based methods for reward maximization is that the effective sample size does not necessarily guarantee true diversity among the samples. As a result, even when the effective sample size is controlled, the generated samples may still lack sufficient diversity.

- **Eliminating Inferior Samples via Global Interaction:** This algorithm involves interactions between batches, allowing the removal of low-quality particles to concentrate resources on more promising ones. A variant of this strategy has also proven effective in autoregressive language models (Zhang et al., 2024).

3.2 Value-Based Importance Sampling

Next, we explain a simple value-based importance sampling approach called SVDD, proposed by Li et al. (2024). For this purpose, we first provide an intuitive overview. This method is iterative in nature. Hence, suppose we are at time t and we have N samples, $\{x_t^{[i]}\}_{i=1}^N$, with uniform weights: $1/N \sum_{i=1}^N \delta_{x_t^{[i]}}$. Following a proposal distribution $q_{t-1}(\cdot|x_t^{[i]})$ (e.g., pre-trained models), we generate M samples $\{x_{t-1}^{[i,j]}\}_{j=1}^M$ for each $x_t^{[i]}$. Ideally, we want to sample from the optimal policy (6). To approximate this, based on importance sampling, we consider the following weighted empirical distribution:

$$\frac{1}{N} \sum_{i=1}^N \sum_{j=1}^M \frac{w_{t-1}^{[i,j]}}{\sum_{j=1}^M w_{t-1}^{[i,j]}} \delta_{x_{t-1}^{[i,j]}}, \quad w_{t-1}^{[i,j]} = \frac{p_{t-1}^*(x_{t-1}^{[i,j]}|x_t^{[i]})}{q_{t-1}(x_{t-1}^{[i,j]}|x_t^{[i]})} = \frac{p_{t-1}^{\text{pre}}(x_{t-1}^{[i,j]}|x_t^{[i]}) \exp(v_{t-1}(x_{t-1}^{[i,j]})/\alpha)}{q_{t-1}(x_{t-1}^{[i,j]}|x_t^{[i]}) \exp(v_{t-1}(x_t^{[i]})/\alpha)}.$$

Since $\exp(v_{t-1}(x_t^{[i]})/\alpha)$ in the above remains constant for all $j \in [1, \dots, M]$, the weight simplifies to

$$w_{t-1}^{[i,j]} = \frac{p_{t-1}^{\text{pre}}(x_{t-1}^{[i,j]}|x_t^{[i]}) \exp(v_{t-1}(x_{t-1}^{[i,j]})/\alpha)}{q_{t-1}(x_{t-1}^{[i,j]}|x_t^{[i]})}. \quad (10)$$

However, repeatedly using this empirical distribution increases the particle size to $O(N^M)$, making it computationally prohibitive. Therefore, we sample to maintain a fixed batch size:

$$\frac{1}{N} \sum_{i=1}^N \delta_{x_{t-1}^{[i]}}, x_{t-1}^{[i]} := x_{t-1}^{[\zeta_i]}, \zeta_i \sim \text{Cat} \left[\left\{ \frac{w_{t-1}^{[i,j]}}{\sum_{k=1}^M w_{t-1}^{[i,k]}} \right\}_{j=1}^M \right].$$

Finally, the complete algorithm is summarized in Algorithm 5.

Differences Between SMC-Based Methods and Value-Based Importance Sampling (SVDD).

While SVDD and SMC share similarities, there are two key differences. First, while the sampling in SMC is performed among the whole batch (i.e., global interaction happens), sampling in SVDD is performed for each sample within a batch independently, with no interaction between samples. Second, the weight definition differs: in SMC, the weight includes $\exp(v_t(\cdot))$ in the denominator, while in SVDD, it does not, as normalization occurs independently for each sample, as mentioned in (10).

Readers may wonder which approach to use. When the goal is alignment (i.e., reward maximization) in Section 1.2.3 (with small α), SVDD is more suitable since SMC may suffer from mode collapse. For conditioning tasks in Section 1.2.1 (with moderate α), the comparison becomes more nuanced. As noted in Section 3.1, SMC benefits from eliminating inferior samples through global interaction, making it advantageous in certain cases.

Algorithm 5 Value-Based Importance Sampling (SVDD) (Li et al., 2024)

- 1: **Require:** Estimated (potentially **non-differentiable**) soft value function $\{\hat{v}_t\}_{t=T}^0$ (Section 2.2), pre-trained diffusion models $\{p_t^{\text{pre}}\}_{t=T}^0$, hyperparameter $\alpha \in \mathbb{R}$, proposal distribution $\{q_t\}_{t=T}^0$, batch size N , duplication size M
- 2: **for** $t \in [T + 1, \dots, 1]$ **do**
- 3: **Importance sampling step:** For $i \in [1, \dots, N]$, get M samples from pre-trained policies $\{x_{t-1}^{[i,j]}\}_{j=1}^M \sim q_{t-1}(\cdot | x_t^{[i]})$. For each $j \in [1, \dots, M]$, calculate

$$w_{t-1}^{[i,j]} := \exp(\hat{v}_{t-1}(x_{t-1}^{[i,j]})/\alpha) \times \frac{p_{t-1}^{\text{pre}}(x_{t-1}^{[i,j]} | x_t^{[i]})}{q_{t-1}(x_{t-1}^{[i,j]} | x_t^{[i]})}.$$

- 4: **Local resampling step:**

$$\forall i \in [1, \dots, N]; \quad x_{t-1}^{[i]} \leftarrow x_{t-1}^{[i, \zeta_{t-1}^{[i]}]}, \quad \zeta_{t-1}^{[i]} \sim \text{Cat} \left(\left\{ \frac{w_{t-1}^{[i,j]}}{\sum_{k=1}^M w_{t-1}^{[i,k]}} \right\}_{j=1}^M \right).$$

- 5: **end for**

- 6: **Output:** $\{x_0^{[i]}\}_{i=1}^N$
-

3.3 Nested-SMC-Based Guidance

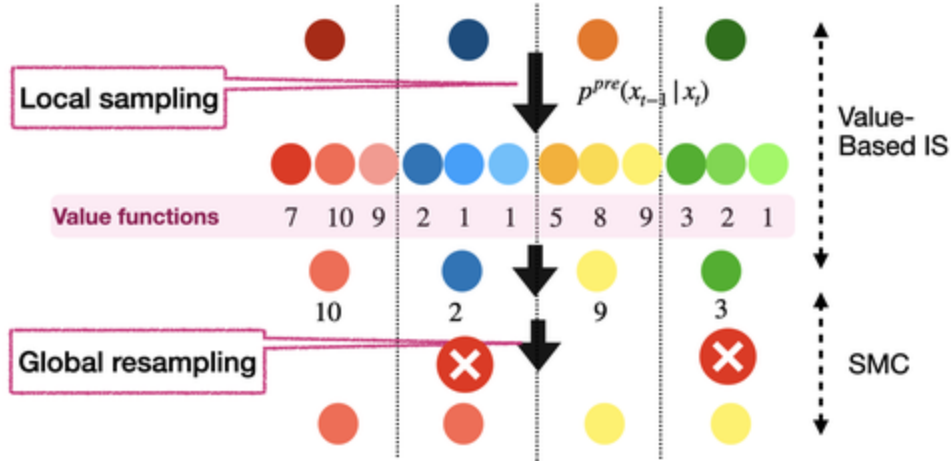


Figure 7: Intuition Behind Nested-SMC-Based Guidance. The algorithm comprises two components: local sampling, which parallels value-based IS sampling, and global resampling, which mirrors SMC-based guidance.

As discussed above, the SMC-based approach and the value-based importance sampling approach each have distinct advantages. A hybrid method, referred to as nested-SMC (or nested-IS) in computational statistics (Naesseth et al., 2019, Algorithm 5), may combine the strengths of both approaches. This method is outlined in Algorithm 6, and the intuition is outlined in Figure 7. Each

step involves two processes: the first is local sampling, resembling value-based importance sampling, and the second is global resampling, characteristic of SMC-based guidance. By incorporating these two elements, nested-IS-based guidance can be more effectively tailored for optimization, allowing the elimination of suboptimal samples through global resampling.

Algorithm 6 Nested-IS-Based Guidance

- 1: **Require:** Estimated (potentially **non-differentiable**) soft value function $\{\hat{v}_t\}_{t=T}^0$ (Section 2.2), pre-trained diffusion models $\{p_t^{\text{pre}}\}_{t=T}^0$, hyperparameter $\alpha \in \mathbb{R}$, proposal distribution $\{q_t\}_{t=T}^0$, batch size N , duplication size M
- 2: **for** $t \in [T + 1, \dots, 1]$ **do**
- 3: **Importance sampling step:** For $i \in [1, \dots, N]$, get M samples from pre-trained policies $\{x_{t-1}^{[i,j]}\}_{j=1}^M \sim q_{t-1}(\cdot | x_t^{[i]})$. And for each $j \in [1, \dots, M]$, and calculate

$$w_{t-1}^{[i,j]} := \exp(\hat{v}_{t-1}(x_{t-1}^{[i,j]})/\alpha) \times \frac{p_{t-1}^{\text{pre}}(x_{t-1}^{[i,j]} | x_t^{[i]})}{q_{t-1}(x_{t-1}^{[i,j]} | x_t^{[i]})}.$$

- 4: **Local resampling step:** $\{x_{t-1}^{[i]}\}_{i=1}^N \leftarrow x_{t-1}^{[i, \zeta_{t-1}^{[i]}]}$ where $\zeta_{t-1}^{[i]} \sim \text{Cat}\left(\left\{\frac{w_{t-1}^{[i,j]}}{\sum_{k=1}^M w_{t-1}^{[i,k]}}\right\}_{j=1}^M\right)$,
- 5: **Calculate global weight (normalizing constant):** $w_{t-1}^{[i]} = 1/M \sum_{j=1}^M w_{t-1}^{[i,j]}$
- 6: **Global resampling step:** Resample by selecting new indices with replacement:

$$\{x_{t-1}^{[i]}\}_{i=1}^N \leftarrow \{x_{t-1}^{\zeta_{t-1}^{[i]}}\}_{i=1}^N, \quad \{\zeta_{t-1}^{[i]}\}_{i=1}^N \sim \text{Cat}\left(\left\{\frac{w_{t-1}^{[i]}}{\sum_{k=1}^N w_{t-1}^{[k]}}\right\}_{i=1}^N\right).$$

- 7: **end for**
 - 8: **Output:** $\{x_0^{[i]}\}_{i=1}^N$
-

3.4 Beam Search for Reward Maximization

Now, consider a special case of reward maximization where it is natural to set $\alpha = 0$. In this scenario, the SVDD algorithm (Algorithm 5) simplifies to Algorithm 7, where the selected index corresponds to the one that maximizes the soft value functions.

This algorithm can also be viewed as a beam search guided by soft value functions. Specifically, multiple nodes are expanded according to the proposal distributions, and the best node is selected based on its value function. While this process may seem greedy, it is not, as soft value functions theoretically serve as look-ahead mechanisms, predicting future rewards from intermediate states.

However, the theoretical foundation of this approach relies on the assumption of perfect soft value function access. In practice, approximation errors may arise, and in certain cases, a deeper search might yield additional benefits. We will later explore deeper search algorithms, such as Monte Carlo Tree Search (MCTS), in Section 6.

Algorithm 7 Beam Search with Soft Value Functions (Li et al., 2024)

- 1: **Require:** Estimated (potentially **non-differentiable**) soft value function $\{\hat{v}_t\}_{t=T}^0$ (refer to Section 2.2), pre-trained diffusion models $\{p_t^{\text{pre}}\}_{t=T}^0$, proposal distribution $\{q_t\}_{t=T}^0$, batch size N , duplication size M
 - 2: **for** $t \in [T + 1, \dots, 1]$ **do**
 - 3: Get M samples from pre-trained policies $\{x_{t-1}^{[i,j]}\}_{j=1}^M \sim p_{t-1}^{\text{pre}}(\cdot | x_t^{[i]})$
 - 4: Update $x_{t-1}^{[i]} \leftarrow x_{t-1}^{[i, \zeta_{t-1}^{[i]}]}$ where $\zeta_{t-1}^{[i]} := \operatorname{argmax}_{j \in [1, \dots, M]} \hat{v}_{t-1}(x_{t-1}^{[i,j]})$.
 - 5: **end for**
 - 6: **Output:** $\{x_0^{[i]}\}$
-

3.5 Selecting Proposal Distributions

Selecting the appropriate proposal distributions is an important decision for the methods introduced so far from Algorithm 4 to Algorithm 7. We outline three fundamental options below.

Pre-Trained Diffusion Policies. The simplest option is to use the policy from the pre-trained diffusion model.

Derivative-Based Guidance. Alternatively, derivative-based guidance from Section 4 can be employed, as demonstrated in Wu et al. (2024); Phillips et al. (2024) with differentiable value function models. Even if the original feedback is non-differentiable and constructing differentiable models is non-trivial, this approach may still outperform pre-trained diffusion models, as the differentiable models can still retain meaningful reward signals.

Fine-Tuned Policies. As we will discuss in Section 9, when we apply distillation or repeat distillation and inference-time techniques, we can use policies from fine-tuned models as enhanced proposal distributions.

4 Derivative-Based Guidance in Continuous Diffusion Models

We have introduced the derivative-free inference-time technique. In this section, we focus on classifier guidance (Dhariwal and Nichol, 2021; Song et al., 2021), a standard derivative-based method in continuous diffusion models. We first provide the intuition underlying the algorithm’s derivation, followed by its formalization within a continuous-time framework. Finally, we propose an algorithm designed for Riemannian diffusion models, which are extensively used in protein structure generation.

Takeaway

Classifier guidance, which adds gradients of value functions at inference time, is derived as an algorithm to approximate the soft optimal policy when discretization errors are negligible. This is formulated within the continuous-time framework using Doob’s transform. For Riemannian diffusion models, this algorithm can be seamlessly extended by incorporating Riemannian gradients instead of standard Euclidean gradients.

4.1 Intuitive Derivation of Classifier Guidance

In this subsection, we derive classifier guidance as a Gaussian policy that approximates the soft-optimal policy.

First, recalling the form of pre-trained policies in diffusion models over Euclidean space, specifically (3) with score parametrization, let us denote the pre-trained model to be

$$p_{t-1}^{\text{pre}}(\cdot | x_t) = \mathcal{N}(\rho^{\text{pre}}(x_t, t); \sigma_t^2 \mathbf{I}), \quad \rho^{\text{pre}}(x_t, t) := x_t + (\delta t) \bar{g}(x_t, t)$$

where

$$\bar{g}(x_t, t) := 0.5x_t + \widehat{\nabla \log p}(x_t; \theta_{\text{pre}}), \quad \sigma_t^2 = (\delta t).$$

Here, (δt) is assumed to be small. Substituting this expression into the optimal policy form in (8) yields

$$\exp\left(\frac{v_{t-1}(x_{t-1})}{\alpha} + \frac{\|x_{t-1} - \rho^{\text{pre}}(x_t, t)\|_2^2}{2\sigma_t^2}\right), \quad (11)$$

up to normalizing constant. However, directly sampling from this policy is challenging; therefore, we consider approximating it.

A natural approach is to approximate this policy with a Gaussian distribution. To achieve this, we apply a Taylor expansion:

$$\exp\left(\frac{v_t(x_t) + \nabla v_t(x_t) \cdot (x_{t-1} - x_t) + O(\|x_{t-1} - x_t\|_2^2)}{\alpha}\right) \times \exp\left(\frac{\|x_{t-1} - x_t - (\delta t) \bar{g}(x_t, t)\|_2^2}{2\sigma_t^2}\right).$$

Since σ_t^2 is much smaller than α (as σ_t^2 scales with (δt)), we can ignore the term $O(\|x_{t-1} - x_t\|_2^2/\alpha)$. Therefore, the expression simplifies to

$$\exp\left(\frac{\|x_{t-1} - x_t - \tilde{\rho}(x_t, t)\|_2^2}{2\sigma_t^2}\right), \quad \tilde{\rho}(x_t, t) = \rho^{\text{pre}}(x_t, t) + \frac{\sigma_t^2 \nabla v_t(x_t)}{\alpha}.$$

Thus, the original policy in (11) is approximated as a Gaussian distribution.

Based on this observation, the complete algorithm is summarized in [Algorithm 8](#), where the gradient of the value function is incorporated at inference time.

Algorithm 8 Classifier Guidance in Continuous Diffusion Models (Dhariwal and Nichol, 2021; Song et al., 2021)

- 1: **Require:** Estimated (**differentiable**) soft value functions $\{\hat{v}_t\}_{t=T}^0$ (refer to Section 2.2), pre-trained diffusion models $\{p_t^{\text{pre}}\}_{t=T}^0$, hyperparameter $\alpha \in \mathbb{R}$
 - 2: **for** $t \in [T + 1, \dots, 1]$ **do**
 - 3:

$$x_{t-1} \sim \mathcal{N} \left(\rho^{\text{pre}}(x_t, t) + \frac{\sigma_t^2 \nabla \hat{v}_t(x_t)}{\alpha}, \sigma_t^2 \right)$$
 - 4: **end for**
 - 5: **Output:** x_0
-

4.2 Derivative-Free Guidance Versus Classifier Guidance

The critical assumption in classifier guidance is that accurate differentiable value function models can be constructed with respect to the inputs. A straightforward scenario for building such models is an inpainting task, where classifier guidance performs effectively. However, in many molecular design tasks, this assumption may not hold, as discussed in the introduction and Section 3. In such cases, derivative-free guidance becomes advantageous, as these methods do not require differentiable rewards or value function models.

It is also worthwhile to note these two approaches (derivative-free guidance and classifier-guidance) can still be combined by employing classifier guidance as a proposal distribution in derivative-free methods, potentially with different value functions. Specifically, even if the differentiable models used in classifier guidance are not fully accurate, they can serve as proposal distributions while SMC-based guidance or value-based sampling leverages more precise non-differentiable value function models, as we discuss in Section 3.5.

4.3 Continuous-Time Formalization via Doob transform

In this section, we formalize the intuitive derivation of classifier guidance in Section 4.1. For this purpose, we explain the continuous-time formulation of diffusion models first.

4.3.1 Preparation

We begin by outlining the fundamentals of diffusion models within the continuous-time framework. For further details, refer to Uehara et al. (2024, Section 1.1.1) or many other reviews (Tang and Zhao, 2024). The training process can be summarized as follows: (1) defining the forward SDE and (2) learning the time-reversal SDE by estimating the score functions.

Forward and Time-Reversal SDE. We first introduce a forward stochastic differential equation (SDE) from $t \in [0, T]$. A widely used example is the variance-preserving (VP) process:

$$t \in [0, T]; dx_t = -0.5x_t dt + dw_t, x_0 \sim p^{\text{pre}}(x), \tag{12}$$

where dw_t denotes standard Brownian motion. Two key observations are:

- As T approaches ∞ , the limiting distribution converges to $\mathcal{N}(0, I)$.
- The time-reversal SDE (Anderson, 1982), which preserves the marginal distribution, is given by:

$$t \in [0, T]; dz_t = [0.5z_t + \nabla \log q_{T-t}(z_t)]dt + dw_t. \quad (13)$$

Here, $q_t \in \Delta(\mathbb{R}^d)$ denotes the marginal distribution at time t induced by the forward SDE (12). Notably, the marginal distribution of z_{T-t} is the same as that of x_t induced by the forward SDE. Note the notation t is reversed relative to the forward SDE in (12).

These observations suggest that with sufficiently large T , starting from $\mathcal{N}(0, I)$ and following the time-reversal SDE (13), we can sample from the data distribution (i.e., p^{pre}) at terminal time T . A key challenge remains in learning the score function $\nabla \log q_{T-t}(z_t)$. In diffusion models, the primary objective is to estimate this score function. For such training methods, refer to Example 1. Our work assumes the availability of a pre-trained model $s(z_t, T - t; \theta_{\text{pre}})$, that predicts $\nabla \log q_{T-t}(z_t)$, fixed after pre-training.

4.3.2 Doob Transform

We now proceed to derive classifier guidance more rigorously. Consider a pre-trained model represented by

$$t \in [0, T]; dz_t = [0.5z_t + s(z_t, T - t; \theta_{\text{pre}})]dt + dw_t, \quad z_0 \sim \delta_{z_0^{\text{ini}}}. \quad (14)$$

We denote the resulting distribution as p^{pre} . The following theorem is instrumental in deriving classifier guidance.

Theorem 2 (Doob Transform). *For a value function: $v_t(\cdot) = \log \mathbb{E}_{\theta_{\text{pre}}}[\exp(r(z_T)) | z_t = \cdot]$ where the expectation $\mathbb{E}_{\theta_{\text{pre}}}[\cdot]$ is induced by the pre-trained model (14), the distribution induced by the SDE:*

$$t \in [0, T]; dz_t = [0.5z_t + \{s(z_t, T - t; \theta_{\text{pre}}) + \nabla \log v_t(z_t)\}]dt + dw_t \quad (15)$$

is a target distribution, proportional to $\exp(r(x))p^{\text{pre}}(x)$.

This theorem implies that, with standard Euler-Maruyama discretization, classifier guidance can be formally derived as in Algorithm 8 (when $\alpha = 1$) such that we can sample from the target distribution $\exp(r(x))p^{\text{pre}}(x)$. Here, we remark that $v_t(\cdot) = \log \mathbb{E}_{\theta_{\text{pre}}}[\exp(r(z_T)) | z_t = \cdot]$ in the theorem serves as the continuous-time analogue of the value function, which we introduce in (6).

The Doob transform is a celebrated result in stochastic processes (e.g., Chetrite and Touchette (2015, Chapter 3)). The connection between classifier guidance and the Doob transform has been highlighted in works such as Zhao et al. (2024); Denker et al. (2024). Furthermore, Uehara et al. (2024); Denker et al. (2024) demonstrated that, in the context of RL-based fine-tuning, the optimal control that maximizes entropy-regularized rewards coincides with the SDE given in (15).

Remark 3. *When the initial distribution p^{ini} from pre-trained models is stochastic, we technically need to change the initial distribution. More specifically, we need to set the initial distribution proportional to $\exp(v_0(x))p^{\text{ini}}(x)$. For details, refer to Uehara et al. (2024).*

4.4 Guidance in Riemannian Diffusion Models

We now extend the discussion from Euclidean spaces to Riemannian manifolds (De Bortoli et al., 2022; Yim et al., 2023; Chen and Lipman, 2023). To do so, we first provide a concise introduction to Riemannian manifolds, focusing specifically on the special orthogonal group (SO(3)). This is because SE(3) (i.e., $SO(3) \otimes \mathbb{R}^3$) is commonly employed in protein conformation generation to efficiently model the 3D coordinates of the protein backbone (Yim et al., 2023; Watson et al., 2023). Subsequently, we describe the corresponding classifier guidance method. For a more detailed introduction to Riemannian manifolds, we refer readers to (Lee, 2018).

4.4.1 Primer: Riemannian Manifolds

We denote a d -dimensional Riemannian submanifold embedded in \mathbb{R}^m by \mathcal{M} . The manifold is a space that locally resembles Euclidean space, and is formally characterized by a local coordinate chart $\phi : \mathcal{M} \rightarrow \mathbb{R}^d$ and its inverse ψ . A key concept in a manifold is the tangent space, which represents the space of possible velocities for a particle moving along the manifold. For each point $x \in \mathcal{M}$, the tangent space $\mathcal{T}_x\mathcal{M}$ is formally defined as the space spanned by the column vectors of the Jacobian $d\psi/d\tilde{x}|_{\tilde{x}=\phi(x)}$. A Riemannian manifold is then defined as a manifold equipped with a specific metric $g : \mathcal{T}_x\mathcal{M} \times \mathcal{T}_x\mathcal{M} \rightarrow \mathbb{R}$, often denoted by $\langle \cdot, \cdot \rangle_g$. An important example in protein design is the well-known SO(3) group.

Example 3 (SO(3)). Consider the set of 3×3 orthogonal matrices, denoted by $SO(3)$. While the intrinsic dimension d is 3, this is embedded in \mathbb{R}^9 . The associated tangent space at x (i.e., $\mathcal{T}_x(SO(3))$) consists of skew-symmetric matrices: $\{xA : A^\top = -A\}$ where the Riemannian metric is defined using the Frobenius inner product: $\langle A_1, A_2 \rangle_g = \text{Tr}(A_1^\top A_2)$. Specifically, the tangent space corresponds to

$$\{x[v_1, v_2, v_3]_\times : v_1 \in \mathbb{R}, v_2 \in \mathbb{R}, v_3 \in \mathbb{R}\}, \quad [v]_\times := \begin{pmatrix} 0 & -v_3 & v_2 \\ v_3 & 0 & -v_1 \\ -v_2 & v_1 & 0 \end{pmatrix}.$$

This can be derived by introducing a curve $x(t) \in SO(3)$ such that $x(0) = x$, and computing the gradient of $x^\top(t)x(t) = I$. The gradient $\nabla x(0)$ satisfies

$$\nabla x(0)^\top \cdot x + x^\top \cdot \nabla x(0) = 0.$$

Then, it is clear $\nabla x(0)$ belongs to $\{xA : A^\top = -A\}$.

We now summarize additional key concepts:

- **Geodesic:** Given a point $x \in \mathcal{M}$ and a velocity $v \in \mathcal{T}_x\mathcal{M}$, the geodesic is defined as a trajectory $\gamma(t) : \mathcal{R} \rightarrow \mathcal{M}$, determined by the initial point x and velocity v :

$$\gamma(0) = x, \quad \left. \frac{d\gamma(t)}{dt} \right|_{t=0} = v, \quad (16)$$

along with the geodesic equation. This trajectory is locally uniquely defined. For example, in Euclidean spaces, it simplifies to $x + tv$. Hence, intuitively, geodesic is the locally shortest path on a Riemannian manifold.

- **Exponential map:** Given $x \in \mathcal{M}$, the exponential map is defined as $\mathcal{T}_x\mathcal{M} : v \rightarrow \gamma(1) \in \mathcal{M}$, where $\gamma(t)$ is the geodesic described above.
- **Logarithmic Map:** The logarithmic map is the inverse of the exponential map.
- **Riemannian Gradient:** The Riemannian gradient of a function $f : \mathcal{M} \rightarrow \mathbb{R}$ at x denoted by $\nabla^g f(\cdot) \in \mathcal{T}_x(\mathcal{M})$ is defined as an element satisfying

$$\forall v \in \mathcal{T}_x\mathcal{M}; \quad \left. \frac{df(\gamma(t))}{dt} \right|_{t=0} = \langle \nabla^g f(x), v \rangle_g,$$

where $\gamma(t)$ is a curve satisfying (16). This reduces to a standard gradient in a Euclidean space.

Now, let's revisit the example of $SO(3)$ to see how these concepts are applied.

Example 3 (continued). Given a point $x \in SO(3)$ and velocity $v \in \mathcal{T}_x(SO(3))$, the exponential map is defined as $x \exp(v)$. Using Rodrigues' rotation formula (Lee, 2018), it can be simplified to

$$x\{I + \sin(\alpha)[v/\|v\|_2]_\times + (1 - \cos(\alpha))\{[v/\|v\|_2]_\times\}^2\},$$

where $\alpha = \|v\|_2$. Then, the Riemannian gradient in $\mathcal{T}_x(SO(3))$ is given by :

$$0.5(\nabla^{\text{Ecu}} f(x) - \{\nabla^{\text{Ecu}} f(x)\}^\top) \quad (17)$$

where ∇^{Ecu} is the Euclidean gradient.

4.4.2 Classifier Guidance in Riemannian Diffusion Models

Algorithm 9 Classifier Guidance in Riemannian Diffusion Models

- 1: **Require:** Estimated (**differentiable**) soft value function $\{\hat{v}_t\}_{t=T}^0$ (refer to Section 2.2), pre-trained diffusion models $\{p_t^{\text{pre}}\}_{t=T}^0$, hyperparameter $\alpha \in \mathbb{R}$
- 2: **for** $t \in [T + 1, \dots, 1]$ **do**
- 3: Calculate the velocity to proceed:

$$\text{vel}_t = (\delta t)\{s(x_t, T - t; \theta_{\text{pre}}) + \nabla^g \hat{v}_t(x_t)/\alpha\} + \sqrt{(\delta t)}\epsilon_t, \quad \epsilon_t \sim \mathcal{N}(0, I_d),$$

where $\mathcal{N}(0, I_d)$ is Gaussian distribution on a Riemannian manifold.

- 4: Move from x_t to x_{t-1} along geodesics:

$$x_{t-1} = \exp_{x_t}[\text{vel}_t]$$

- 5: **end for**
 - 6: **Output:** x_0
-

Now, with the above preparation, the pre-trained model is defined as an SDE on a manifold \mathcal{M} :

$$t \in [0; T]; \quad dx_t = s(x_t, T - t; \theta_{\text{pre}})dt + dw_t^{\mathcal{M}},$$

where $dw_t^{\mathcal{M}}$ denotes Brownian motion on a Riemannian manifold \mathcal{M} . The discretization is given by:

$$x_{t-1} = \exp_{x_t}[\text{vel}_t], \text{vel}_t = (\delta t)s(x_t, T - t; \theta_{\text{pre}}) + \sqrt{(\delta t)}\epsilon_t, \quad \epsilon_t \sim \mathcal{N}(0, I_d),$$

where ϵ_t is a normal distribution on the manifold \mathcal{M} . Each step thus consists of two operations: (1) calculating the tangent (velocity) vel_t in the tangent space at x_t and (2) moving along the geodesic induced by the velocity vel_t , starting at x_t . In the Euclidean case, the second step reduces to $x_t + \text{vel}_t$.

Classifier Guidance. Now, we extend classifier guidance to Riemannian manifolds. Similar to the Euclidean case, we calculate a Riemannian gradient at each time step during inference and incorporate it into the velocity. The updated velocity becomes:

$$(\delta t)\{s(x_t, T - t; \theta_{\text{pre}}) + \underbrace{\nabla^g v(x_t)/\alpha}_{\text{Additional Riemannian gradient}}\} + \sqrt{(\delta t)}\epsilon_t.$$

For example, in the case of $SO(3)$, the Riemannian gradient is computed using (17).

The complete algorithm is summarized in [Algorithm 9](#). Note this approach can be formalized using Doob’s theorem for Riemannian manifolds, as discussed in [Section 4.3](#).

5 Derivative-Based Guidance in Discrete Diffusion Models

We now focus on inference-time techniques specifically designed for discrete diffusion models. In [Section 2.1](#), we highlighted that exact sampling from the optimal policy is feasible within discrete diffusion models under certain limited scenarios. Here, we revisit this point by demonstrating that exact sampling from the optimal policy can be achieved through polynomial-time computation of value functions. Building on this point, we explain derivative-based guidance following the approach of [Nisonoff et al. \(2024\)](#). Finally, we formalize the discussion within a continuous-time framework ([Wang et al., 2024](#)).

Takeaways

In discrete diffusion, while the original action space grows exponentially with respect to token length, the nominal action space is polynomial, allowing optimal policies to be sampled with polynomial computation of value functions. This argument has been formalized using Doob’s transform in the continuous-time formulation.

Despite this, polynomial computation remains computationally expensive in many practical scenarios. One approach to mitigate this issue is to employ derivative-based guidance.

5.1 Exact Sampling in Discrete Diffusion Models

Our objective in this subsection is to show that sampling from the optimal policy can be achieved with polynomial-time computation of value functions in discrete diffusion models. As a preliminary step, we demonstrate that the effective action space in the pre-trained policy scales *polynomially*

with respect to token length, rather than *exponentially*. We then extend this argument to show that the effective action space in the optimal policy also scales polynomially. This leads to the conclusion that sampling from the optimal policy is computationally feasible using polynomial computation, avoiding the need for exponential computation of value functions.

Closer look at policies from pre-trained models. Our first objective here is to demonstrate that the effective action space in discrete diffusion models is LK rather than K^L , where L is the token length and K is the vocabulary size.

To begin, recall that the pre-trained policy in diffusion models is expressed as:

$$\prod_{l=1}^L p_{t-1}^{\text{pre}}(x_{t-1}^l | x_t^{1:L}), \text{ where } p_{t-1}^{\text{pre}}(x_{t-1}^l | x_t^{1:L}) := \mathbb{I}(x_t^l = x_{t-1}^l) + Q_{x_{t-1}^l, x_t^{1:L}}^{\text{pre}}(t)(\delta t), \quad (18)$$

where (δt) is a discretization step. For example, in maskd diffusion models mentioned (Example 2),

$$Q_{x_{t-1}^l, x_t^{1:L}}^{\text{pre}}(t) := \begin{cases} \frac{\alpha_{t-1} - \alpha_t}{1 - \bar{\alpha}_t} \hat{x}_0(x_t; \theta^{\text{pre}}) & \text{when } x_{t-1}^l \neq x_t^l, x_t^l = \mathbf{Mask} \\ - \sum_{z \neq x_t^l} Q_{z, x_t^{1:L}}^{\text{pre}}(t) & \text{when } x_{t-1}^l = x_t^l, x_t^l = \mathbf{Mask}, \\ 0 & \text{when } x_t^l \neq \mathbf{Mask}. \end{cases}$$

At first glance, evaluating the optimal policy based on the pre-trained policy (18), i.e.,

$$\exp(v(x_{t-1}^{1:L})) \prod_{l=1}^L p_{t-1}^{\text{pre}}(x_{t-1}^l | x_t^{1:L})$$

might seem computationally prohibitive, as it appears to require $O(L^K)$ evaluations of the value functions. However, it can actually be computed using only $O(LK)$ operations. The key idea lies in identifying an asymptotically equivalent policy, as described below.

- **Case 1: A single Token Change.** Consider the scenario where only a single token (position $c \in 1, \dots, L$) changes in x_{t-1}^l . The transition probability is:

$$p_{t-1}^{\text{pre}}(x_{t-1}^{1:L} | x_t^{1:L}) = Q_{x_{t-1}^c, x_t^{1:L}}^{\text{pre}}(t)(\delta t) \times \prod_{l \neq c} \left\{ 1 + Q_{x_{t-1}^l, x_t^{1:L}}^{\text{pre}}(t)(\delta t) \right\}.$$

By some algebra, we can approximate this as:

$$p_{t-1}^{\text{pre}}(x_{t-1}^{1:L} | x_t^{1:L}) = \underbrace{Q_{x_{t-1}^c, x_t^{1:L}}^{\text{pre}}(t)(\delta t)}_{O(\delta t)\text{term (first order)}} + O((\delta t)^2).$$

- **Case 2: Multiple Token Changes.** When multiple tokens change in x_{t-1}^l , similar calculations yield $p_{t-1}^{\text{pre}}(x_{t-1}^{1:L} | x_t^{1:L}) = O((\delta t)^{\text{Ch}(x_{t-1}^{1:L}, x_t^{1:L})})$ where Ch denotes the number of token changes between $x_{t-1}^{1:L}$ and $x_t^{1:L}$, defined as $\text{Ch}(x_{t-1}, x_t) := \|x_{t-1} - x_t\|_1/2$.

Summarizing the above, ignoring second-order terms, the resulting asymptotically equivalent policy becomes:

$$p_{t-1}^{\text{pre}}(x_{t-1}^{1:L} | x_t^{1:L}) = \begin{cases} 0, & \text{Ch}(x_{t-1}^{1:L}, x_t^{1:L}) \geq 2, \\ Q_{x_{t-1}^{1:L}, x_t^{1:L}}^{\text{pre}}(t)(\delta t), & \text{Ch}(x_{t-1}^{1:L}, x_t^{1:L}) = 1, \\ 1 + Q_{x_{t-1}^{1:L}, x_t^{1:L}}^{\text{pre}}(t)(\delta t), & \text{Ch}(x_{t-1}^{1:L}, x_t^{1:L}) = 0, \end{cases} \quad (19)$$

where $Q_{x_{t-1}^{1:L}, x_t^{1:L}}^{\text{pre}}(t)$ in the second line implicitly means $Q_{x_{t-1}^c, x_t^{1:L}}^{\text{pre}}(t)$ where c is the changed token place, and the generator in the third line is

$$Q_{x_t^{1:L}, x_t^{1:L}}^{\text{pre}}(t) = - \sum_{\{x'_{t-1}: x'_{t-1} \neq x_t^{1:L}, \text{Ch}(x'_{t-1}, x_t^{1:L})=1\}} Q_{x'_{t-1}, x_t^{1:L}}^{\text{pre}}(t).$$

Crucially, since the effective action space in x_{t-1} is LK (instead of exponential in L), the computational cost of the above summation only requires LK operations, ensuring polynomial complexity.

Sampling from the Optimal Policy. Now, let us revisit the formulation of the optimal policy. For simplicity, we denote $x_{t-1}^{1:L}$ as x_{t-1} . Substituting (19) into the form of the optimal policy (8), we obtain:

$$p_{t-1}^*(x_{t-1} | x_t) = \begin{cases} 0, & \text{Ch}(x_{t-1}, x_t) \geq 2, \\ \frac{\exp(v_{t-1}(x_{t-1}))Q_{x_{t-1}, x_t}^{\text{pre}}(t)(\delta t)}{\exp(v_{t-1}(x_t))\{1+Q_{x_t, x_t}^{\text{pre}}(t)(\delta t)\} + \sum_{x'_{t-1}} \exp(v_{t-1}(x'_{t-1}))Q_{x'_{t-1}, x_t}^{\text{pre}}(t)(\delta t)}, & \text{Ch}(x_{t-1}, x_t) = 1, \\ \frac{\exp(v_{t-1}(x_t))\{1+Q_{x_t, x_t}^{\text{pre}}(t)(\delta t)\}}{\exp(v_{t-1}(x_t))\{1+Q_{x_t, x_t}^{\text{pre}}(t)(\delta t)\} + \sum_{x'_{t-1}} \exp(v_{t-1}(x'_{t-1}))Q_{x'_{t-1}, x_t}^{\text{pre}}(t)(\delta t)}, & \text{Ch}(x_{t-1}, x_t) = 0. \end{cases}$$

This formulation may seem complex, so let's simplify it.

For the case when $\text{Ch}(x_{t-1}, x_t) = 1$, the expression simplifies to:

$$\frac{\exp(v_{t-1}(x_{t-1}))Q_{x_{t-1}, x_t}^{\text{pre}}(t)(\delta t)}{\exp(v_{t-1}(x_t))} + O((\delta t)^2).$$

Ignoring higher-order terms $O((\delta t)^2)$, we can further streamline the formulation. The complete algorithm is summarized in [Algorithm 10 \(Nisonoff et al., 2024\)](#).

The key takeaway is that we can again avoid the curse of token length, as the computational cost of evaluating the value function remains LK . However, in practical applications, even this computational cost may be prohibitive. To address this, two approximation strategies can be employed:

- **SMC-Based Guidance (Section 3.1) or Value-Based Sampling (Section 3.2)** : These methods are more feasible in practice. Notably, even the value-based sampling described in [Section 3](#) requires only M evaluations of the value function, a significant reduction compared to LK .
- **Derivative-Based Approximation (Nisonoff et al., 2024; Vignac et al., 2023)**: In the next section, we introduce a further reduction technique by computing derivatives of the value functions, effectively minimizing the LK computation overhead.

Remark 4 (Combination with More Advanced Discretization Methods). *We have employed the most basic discretization method to define policies. However, many state-of-the-art approaches could potentially be applied for policy distillation (Campbell et al., 2022; Ren et al., 2024; Zhao et al., 2024).*

Algorithm 10 Classifier Guidance in Discrete Diffusion Models (Nisonoff et al., 2024)

- 1: **Require:** Estimated (**potentially nondifferentiable**) soft value function $\{\hat{v}_t\}_{t=T}^0$ (refer to Section 2.2), pre-trained diffusion models
- 2: **for** $t \in [T + 1, \dots, 1]$ **do**
- 3: Sample from the following:

$$p_{t-1}^*(x_{t-1} \mid x_t) = \begin{cases} 0, & (\text{Ch}(x_{t-1}, x_t) \geq 2), \\ \frac{\exp(\hat{v}_{t-1}(x_{t-1}))Q_{x_{t-1}, x_t}^{\text{pre}}(t)(\delta t)}{\exp(\hat{v}_{t-1}(x_t))}, & (\text{Ch}(x_{t-1}, x_t) = 1), \\ 1 - \sum_{\{x'_{t-1}: \text{Ch}(x'_{t-1}, x_t)=1\}} \frac{\exp(\hat{v}_{t-1}(x'_{t-1}))Q_{x'_{t-1}, x_t}^{\text{pre}}(t)(\delta t)}{\exp(\hat{v}_{t-1}(x_t))} & (\text{Ch}(x_{t-1}, x_t) = 0). \end{cases}$$

- 4: **end for**
 - 5: **Output:** x_0
-

5.2 Derivative-Based Guidance in Discrete Diffusion Models

As we did in Section 4.1, we perform a Taylor expansion using a one-hot representation. For the case where $\text{Ch}(x_{t-1}, x_t) = 1$, the expression becomes:

$$\frac{\{\exp(v_t(x_t)) + \nabla \exp(v_t(x_t)) \cdot (x_{t-1} - x_t) + O(\|x_{t-1} - x_t\|_2^2)\}}{\exp(v_t(x_t))} \times Q_{x_{t-1}, x_t}^{\text{pre}}(t)(\delta t),$$

where x_t is embedded into a $L \times K$ dimensional one-hot representation. By ignoring the higher-order terms $O(\|x_{t-1} - x_t\|_2^2)$, this simplifies to:

$$Q_{x_{t-1}, x_t}^{\text{pre}}(t) \{1 + \nabla v_t(x_t) \cdot (x_{t-1} - x_t)\}(\delta t). \quad (20)$$

Nisonoff et al. (2024) proposed this approximation as a practical implementation of classifier guidance in discrete diffusion models. This procedure is summarized in Algorithm 11.

Remark 5. *Another asymptotically equivalent formulation of (20) is $Q_{x_{t-1}, x_t}^{\text{pre}}(t) \exp(\nabla v_t(x_t) \cdot (x_{t-1} - x_t))(\delta t)$ noting $\exp(x) \approx 1 + x$ when x is small.*

However, it is important to note that this practical version could have a potential issue. Most notably, in discrete spaces, formal derivatives cannot be done, rendering the Taylor expansion technically invalid. Consequently, unlike in continuous domains, the derivative-based approach lacks formal guarantees in discrete spaces.

Algorithm 11 Classifier Guidance with Taylor Approximation in Discrete Diffusion Models (Nisonoff et al., 2024)

- 1: **Require:** Estimated (**differentiable**) soft value function $\{\hat{v}_t\}_{t=T}^0$ (refer to Section 2.2), pre-trained diffusion models
- 2: **for** $t \in [T + 1, \dots, 1]$ **do**
- 3: Define the following generator:

$$Q_{x_{t-1}^l, x_t^{1:L}}^{\text{new}}(t) := Q_{x_{t-1}, x_t}^{\text{pre}}(t) \{1 + [\nabla \hat{v}_t(x_t^{1:L})]_l \cdot (x_{t-1}^l - x_t^l)\} \text{ (if } x_{t-1}^l \neq x_t^l)$$

$$Q_{x_{t-1}^l, x_t^{1:L}}^{\text{new}}(t) := - \sum_{x_{t-1}^l \neq x_t^l} Q_{x_{t-1}, x_t}^{\text{new}}(t) \text{ (if } x_{t-1}^l = x_t^l)$$

- 4: Sample from

$$\prod_{l=1}^L p_{t-1}^{\text{gui}}(x_{t-1}^l | x_t^{1:L}), \text{ where } p_{t-1}^{\text{gui}}(x_{t-1}^l | x_t^{1:L}) := \mathbb{I}(x_t^l = x_{t-1}^l) + Q_{x_{t-1}, x_t}^{\text{new}}(t)(\delta t).$$

- 5: **end for**
 - 6: **Output:** $x_0^{1:L}$
-

5.3 Continuous-Time Formalization via Doob Transform

We now formalize the classifier guidance method for discrete diffusion models in continuous time formulation, as outlined in Section 5.1. To do so, we first need to understand how discrete diffusion models are framed within the continuous-time formulation. Finally, we formalize the classifier guidance method for diffusion models using the Doob transform in continuous-time Markov chains (CTMC).

5.3.1 Preparation

The training of discrete diffusion models follows the same principles as Euclidean diffusion models. We define the forward noising process and aim to learn the denoising process. However, in discrete diffusion models, we must account for the transition from Brownian motion to continuous-time Markov chains (CTMC). Due to this difference, the “score” is replaced with the “ratio”. This substitution is expected, as ratio matching is a well-established method for estimating unnormalized models with discrete data (Hyvärinen, 2007), similar to how score matching is widely used for continuous data (Hyvärinen and Dayan, 2005).

Forward and Time-Reversal SDE. We consider the following family of distributions $q_t \in \mathbb{R}^K$ (a vector summing to 1), which evolves from $t = 0$ to $t = T$ according to a CTMC:

$$\frac{dq_t}{dt} = Q(t)q_t, \quad p_0 \sim p_{\text{data}},$$

where $Q(t) \in \mathbb{R}^{K \times K}$ is the generator. Typically, q_t is designed to converge toward a simple limiting distribution as $t \rightarrow T$. A common strategy is to introduce a *mask* into \mathcal{X} and gradually mask a sequence so that the limiting distribution becomes fully masked (Shi et al., 2024; Sahoo et al., 2024).

Specifically, these works define the forward masking process so that $q_t \sim \text{Cat}(\bar{\alpha}_t x_t + (1 - \bar{\alpha}_t) \mathbf{m})$ as we saw in Example 2.

Now, we consider the time-reversal CTMC (Sun et al., 2022), which preserves the marginal distribution. This can be expressed as follows:

$$\frac{dq_{T-t}}{dt} = \bar{Q}(T-t)q_{T-t}, \quad \bar{Q}_{y,x}(t) = \begin{cases} \frac{q_t(y)}{q_t(x)} Q_{x,y}(t) & (y \neq x), \\ -\sum_{z \neq x} \bar{Q}_{z,x}(t) & (y = x), \end{cases}$$

where $Q_{y,x}(t)$ is a (y, x) -entry of a generator $Q(t)$. This formulation implies that if we can learn the marginal density ratio $q_t(y)/q_t(x)$, we can sample from the data distribution at $t = T$ by following the above CTMC governed by $\bar{Q}(T-t)$. For details on training this ratio, see Lou et al. (2023). In the subsequent discussion, we assume that the pre-training phase is complete and a pre-trained discrete diffusion model is available.

5.3.2 Doob Transform in CTMC

We are now prepared to formally derive classifier guidance in discrete diffusion models. Assume we have a pre-trained model characterized by the generator $Q^{\text{pre}}(t)$:

$$\frac{dz_t}{dt} = Q^{\text{pre}}(t)z_t, \quad z_0 \sim \delta(z_0^{\text{ini}}).$$

The distribution generated by the above CTMC corresponds to p^{pre} , which characterizes the natural-like design space. Note that time 0 represents the noise and time T represents the terminal here.

With the above preparation, we present the following key theorem: Doob transform in CTMC.

Theorem 3 (Doob transform (From Theorem 1, 2 in Wang et al. (2024))). *Define the soft value functions as $v_t(\cdot) := \log \mathbb{E}_{Q^{\text{pre}}}[\exp(r(z_T)) | z_t = \cdot]$ where the expectation is taken with respect to the distribution induced by the pre-trained model. Then, the distribution induced by the CTMC:*

$$\frac{dz_t}{dt} = Q^*(t)z_t, \quad Q_{x,y}^*(t) = Q_{x,y}^{\text{pre}}(t) \exp(\{v_t(y) - v_t(x)\}), \quad (21)$$

is the target distribution, proportional to the target distribution $\exp(r(x))p^{\text{pre}}(x)$.

This theorem indicates that, using standard Euler-Maruyama discretization, we can derive the classifier guidance algorithm introduced in Algorithm 10 such that we can sample from the target distribution. Here, we remark that $v_t(\cdot) := \log \mathbb{E}_{Q^{\text{pre}}}[\exp(r(z_T)) | z_t = \cdot]$ is seen as the continuous-time analog of the value function in (6).

The Doob transform for CTMCs is well-established in the literature on the stochastic process (e.g., Levin and Peres (2017, Chapter 17); Chetrite and Touchette (2015, Chapter 3)). In the context of guidance for discrete diffusion models, Nisonoff et al. (2024) and Wang et al. (2024) introduce this form. Notably, Wang et al. (2024) also proves that, in the context of RL-based fine-tuning, the above CTMC in (21) maximizes the entropy-regularized reward objective.

6 Tree Search Algorithms for Alignment

A promising approach for more accurate inference alignment involves leveraging search-based algorithms. As outlined in Section 3.4, SVDD in Li et al. (2024) performs beam search using a value function. More sophisticated algorithms, such as Monte Carlo Tree Search (MCTS) (Kocsis and Szepesvári, 2006; Silver et al., 2016; Hubert et al., 2021; Xiao et al., 2019), can also be applied to diffusion models by appropriately defining the search tree. Key aspects to address include determining the depth and width of the search tree, followed by the evaluation of leaf nodes.

Before delving into these aspects in detail, we observe that, unlike in language models (Feng et al., 2023; Hao et al., 2023), relatively few studies (e.g., Li et al. (2024)) have explored this direction within the context of diffusion models. Given the success of MCTS in molecular generation (Yang et al., 2017; Kajita et al., 2020; Yang et al., 2020; Swanson et al., 2024) in general, we believe that this approach offers considerable potential for molecular design even when using diffusion models. We encourage further research in this area.

Key Message in Section 6

Pre-trained diffusion models inherently induce a tree structure that characterizes natural-like designs. Search algorithms, such as Monte Carlo Tree Search (MCTS), can be applied to maximize rewards while effectively utilizing value functions.

6.1 Defining the Search Tree

We now discuss how to properly define the search tree.

Original Tree Depth/Width. In diffusion models, a natural approach is to set the original tree depth according to the discretization level, typically ranging from 50 to 1000. However, the original tree width in diffusion models is considerably larger. For example, in continuous diffusion, the action space lies in a high-dimensional Euclidean space, making exhaustive search computationally prohibitive. Even in masked discrete diffusion models, the tree width is LK (as we mention in Section 5.1), where L denotes the token length and K the vocabulary size.

Search Tree Depth/Width. The primary challenge lies in managing the large tree width and depth discussed above. To address this, we must adopt search algorithms capable of strategically limiting node expansion and constraining both the width and depth of the tree. Specifically, starting from the root node (the current state during inference), we limit the tree width and depth by sampling nodes from pre-trained models during expansion, preventing further growth beyond a specified limit. This subsampling strategy, which leverages pre-trained models, has been effectively used in RL like AlphaZero and its variants (Hubert et al., 2021; Grill et al., 2020), as well as in language models (Feng et al., 2023; Hao et al., 2023).

6.2 How to Run Simulations from Leaf Nodes

While any off-the-shelf search algorithm can be applied to the tree described above, a key decision is how to evaluate the leaf node in the search tree (i.e., the simulation phase in MCTS). To explain it, in the following, let us assume the leaf node is x_{t-1} .

The simplest way to evaluate the leaf node is by using a value function approximation, such as the posterior mean approximation in [Section 2.2](#), and setting it as $r(\hat{x}_0(x_{t-1}))$. However, as t increases, this approximation generally becomes less accurate. A potentially more effective strategy is to evaluate $r(\hat{x}_0(x_{t-k}))$ after running the pre-trained model for an additional k steps. This approach can yield a more precise estimate, as $t-k$ is closer to 0. The algorithm, combined with beam search, is illustrated in [Figure 8](#).

However, it is important to note that this k -step look-ahead incurs additional computational costs. In the extreme case, running the model for t steps would provide the most accurate evaluation of $r(x_0)$ at time 0 but would be computationally prohibitive. We leave the exploration of this trade-off between accuracy and computational efficiency for future work.

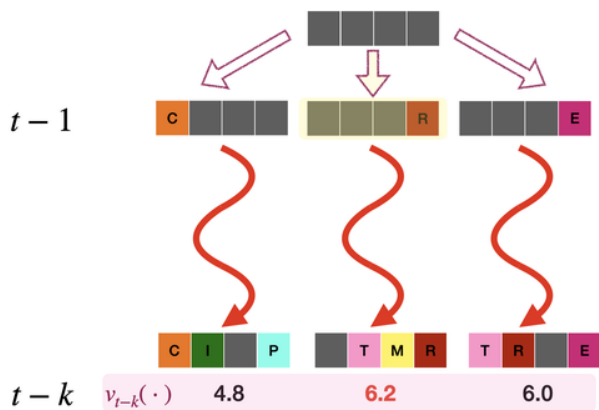


Figure 8: Evaluation of leaf nodes with estimated value functions at $t-k$ rather than $t-1$ by further rolling out pre-trained policies.

7 Editing and Refinement with Diffusion Models

Thus far, we have focused on inference-time techniques that generate samples from scratch, progressing from a noise state (at $t = T$) to the final state (at $t = 0$). In this section, we aim to address two practical scenarios:

- *Editing*: Particularly in biological sequence design, our task is often to *edit* an existing sequence while preserving its original properties and enhancing its target properties. For instance, in antibody design, the typical number of mutations is limited to 5 – 10 ([Bachas et al., 2022](#)). In such cases, the inference-time techniques discussed so far cannot be directly applied.
- *Refinement*: Another closely related motivation is the refinement of generated designs. Even when designs are generated from complete noise using inference-time techniques, we may want to *refine* these designs further. Note that many decoding algorithms for BERT-style models have been developed with this objective in mind, such as Gibbs sampling ([Wang and Cho, 2019](#); [Miao et al., 2019](#)).

In the following sections, we describe how inference-time techniques introduced so far can be adapted for tasks involving editing or refinement.

Key Message in [Section 7](#)

Inference-time techniques can be applied to the editing or refinement of designs by incorporating mutation steps within an evolutionary algorithm.

7.1 Iterative Refinement in Diffusion Models

Algorithm 12 Iterative Refinement for Reward Optimization in Diffusion Models

- 1: **Require:** Estimated soft value function $\{\hat{v}_t\}_{t=0}^T$ (refer to [Section 2.2](#)), pre-trained diffusion models $\{p_t^{\text{pre}}\}_{t=0}^T$ and an initial sequence $x_0^{(0)}$ (the index $\langle \cdot \rangle$ means the number of iteration steps).
 - 2: **for** $s \in [0, \dots, S - 1]$ **do**
 - 3: Sample $x_k^{(s+1)}$ from $q_k(\cdot | x_0^{(s)})$ where q_k is a pre-defined noising policy from x_0 to x_k .
 - 4: Use inference-time techniques introduced so far (methods in [Section 3](#), [Section 4](#)), which combine value function and pre-trained models to obtain $x_0^{(s+1)}$, starting from $x_k^{(s+1)}$
 - 5: (Optional): Filter designs that meet the specified constraints.
 - 6: **end for**
 - 7: **Output:** $\{x_0^{(S)}\}$
-

Here, we present an editing-type algorithm designed for reward optimization with diffusion models, summarized in [Algorithm 12](#).

The algorithm iteratively performs the following steps:

1. Noising: Add noise from x_0 to x_k for some $k \in [0, T]$.
2. Inference-time alignment: Use inference-time technique to transition back from x_k to x_0 .
3. Selection: Retain only the designs that achieve high target rewards and satisfy specific constraints. For example, constraints could include an edit distance threshold relative to predefined seed sequences.

As a special case, when $k = T + 1$, the algorithm reduces to the previously introduced inference-time techniques. However, in this scenario, the algorithm may perform poorly if the constraints are difficult to satisfy. By selecting a moderate k closer to 0, it is possible to generate samples that better adhere to the given constraints.

7.2 Connection with Evolutionary Algorithms

Interestingly, we point out that [Algorithm 12](#) can be viewed as a variant of evolutionary algorithms ([Branke, 2008](#)). Recall that a standard evolutionary algorithm iteratively follows the two steps below:

- **Mutation:** Generate candidate sequences based on the current designs (e.g., by introducing noise).
- **Selection:** Retain only those designs that achieve high target rewards and satisfy the given constraints. For example, constraints could include an edit distance threshold relative to predefined seed sequences.

In our context, it is evident that the mutation step corresponds to the first stage of our algorithm. However, [Algorithm 12](#) adopts a more strategic mutation approach by leveraging inference-time techniques instead of random mutations to generate candidate sequences. This incorporation of inference-time techniques significantly enhances the efficient exploration of natural-like designs.

8 Comparison with Inference-Time Techniques in Language Models

This section examines the connections and distinctions between guidance methods in diffusion models and language models. We begin by comparing diffusion models with autoregressive language models, such as GPT (Brown, 2020), and then proceed to discuss comparisons with masked language models, such as BERT (Kenton and Toutanova, 2019). The key message is as follows.

Key Message

- Most of the guidance methods discussed so far can be directly applied to autoregressive models. However, in autoregressive models, training-free approaches to approximate value functions cannot be utilized due to the lack of forward policies. Additionally, continuous-time formulations play a minimal role within this context.
- Recall that masked diffusion models can be viewed as hierarchical versions of masked language models. Compared to standard masked language models, masked diffusion models are less susceptible to distributional shifts between training and inference phases. By leveraging this connection, we can develop guidance methods in masked language models by drawing analogies to diffusion models.

8.1 Inference-Time Alignment Technique in Autoregressive Models

In the context of autoregressive pre-trained models, which are prevalent in language models, approaches analogous to derivative-free guidance (Section 3) and derivative-based guidance (Section 4) have been explored. These methods are summarized in Table 1. While we acknowledge the significant similarities between autoregressive models and diffusion models, we highlight key properties unique to diffusion models that are not accessible in autoregressive models, as discussed below.

8.1.1 Properties Leveraged in Diffusion Models

We highlight three fundamental properties of diffusion models that distinguish them from autoregressive models in the construction of inference-time algorithms.

Existence of Forward Noising Processes. The training of diffusion models employs a forward process (noising process) from x_0 to x_t , which proves useful not only during training but also in post-training techniques like policy distillation (as discussed in Section 9.2) and pure distillation methods (Salimans and Ho, 2022).

Training-Free Value Functions. Due to the abovementioned forward noising processes, in diffusion models, a one-step denoising mapping from x_t to x_0 (as outlined in Example 1, 2) simplifies the approximation of value functions due to its training-free nature. In contrast, autoregressive models lack such direct mappings and typically rely on Monte Carlo regression or soft Q-learning

Table 1: Examples of corresponding methods between diffusion models and autoregressive models

Algorithm	Diffusion models	Autoregressive models
SMC-based guidance	Section 3.1	Zhao et al. (2024); Lew et al. (2023)
Value-based sampling	Section 3.4	Yang and Klein (2021); Deng and Raffel (2023); Mudgal et al. (2023); Han et al. (2024); Khanov et al. (2024)
Derivative-based guidance	Section 4, 5	Dathathri et al. (2019); Qin et al. (2022) (Plug-in-play approach)
MCTS	Section 6	Leblond et al. (2021); Feng et al. (2023)

(Section 2.2) to construct value functions, adding significant complexity (Han et al., 2024; Mudgal et al., 2023).

Utility of Continuous-Time Formulation. In autoregressive models, plug-and-play methods add gradients of classifiers or rewards at inference time (Dathathri et al., 2019; Qin et al., 2022). While classifier guidance in diffusion models serves a similar purpose, the continuous-time formulation discussed in Section 4 or Section 5 provides a more formal framework for diffusion models. This formulation is critical in constructing several algorithms and foundations in derivative-based guidance.

8.2 Inference-Time Alignment in Masked Language Models

In masked language models, we create inputs with a certain probability of masking and aim to train neural networks (encoders) to demask, i.e., predict the original inputs from the masked ones. Compared to autoregressive language models, masked models are known for their strengths in representation learning, which has led to their widespread use in biology. While lower masking rates are typically employed to capture good representations by understanding global contexts, modern masked language models in biology, such as ESM3 (Hayes et al., 2024) or masked autoencoders for images (He et al., 2022) use more aggressive masking rates to enhance their generative capabilities as well.

As noted in Example 2, masked language models are closely related to masked diffusion models. We will explore these similarities and differences in detail. Then, we discuss alignment methods in masked language models.

8.2.1 Similarities and Differences Compared to Masked Diffusion Models

Both training approaches between masked diffusion models and masked language models are fundamentally similar, although the masking rate in masked language models is typically much

lower. The key distinction lies in the decoding approach as follows.

Masked Diffusion Models. In masked diffusion models, the decoding process is mathematically structured to ensure that the marginal distributions of the “noised distributions” (induced by q_t from $t = 0$ to $t = T$ in Example 2) and the “denoised distributions” (induced by p_t from $t = T$ to $t = 0$ in Example 2) are identical. Hence, since this implies that the training distribution and test distribution at inference time are similar, the learned encoder (neural networks mapping x_t to x_0) avoids distributional shifts. Relatedly, the likelihood of a sample, which plays a crucial role in biological applications such as variant effect prediction (Livesey and Marsh, 2023) or as a key measure to characterize fitness (naturalness) (Hie et al., 2024), can be formally computed using the ELBO bound. This bound offers a formal guarantee in the sense that, in the continuous-time limit as T approaches infinity and with an ideal nonparametric neural network, it is tightly achieved. More specifically, when $T \rightarrow \infty$, recalling (4), it is approximated by

$$\int_{t=0}^{t=1} \mathbb{E}_{x_t \sim q_t(\cdot|x_0)} \left[\frac{\bar{\alpha}'_t}{1 - \bar{\alpha}_t} \mathbb{I}(x_t = \mathbf{Mask}) \log \langle x_0, \log \hat{x}_0(x_t) \rangle \right] dt.$$

Masked Language Models. In masked language models, specific positions to unmask must be defined, with various decoding approaches available, such as confidence-based decoding, left-to-right decoding, and random decoding. While these decoding methods bear certain similarities to masked diffusion models, in which inputs are progressively masked, no universally prescribed approach exists.

Even when a particular decoding method is selected, distributional shift remains a potential issue, as the learned encoder may not accurately reflect the distribution induced by the chosen decoding strategy (i.e., a mismatch between the training and inference-time distributions). Additionally, “formally” calculating the likelihood is challenging, as it is dependent on the decoding method. Given a sequence with $x^{1:L}$, standard approximation techniques include pseudo-likelihood estimation (Miao et al., 2019):

$$\sum_{i=1}^L \log p(x^i | (x^{1:L} \setminus x^i)),$$

where $(x^{1:L} \setminus x^i)$ denotes the sequence $x^{1:L}$ with the i -th token replaced by a masked token. Another way is to use Monte Carlo sampling across multiple decoding strategies:

$$\frac{1}{|\mathcal{G}|} \sum_{\sigma \in \mathcal{G}} \sum_{i=1}^L \log p(x^{\sigma(1)\sigma(2)\dots\sigma(i)} | x^{\sigma(1)\sigma(2)\dots\sigma(i-1)}),$$

where \mathcal{G} is a set that consist of permutation among L tokens. However, these methods lack formal guarantees or could easily suffer from distributional shift.

8.2.2 Adaptation of Alignment Methods

Various decoding methods have been extensively explored in masked language models (Miao et al., 2019; Wang and Cho, 2019). However, to the best of the author’s knowledge, inference-time

alignment methods have received less attention, partly due to the recent success of autoregressive models over masked language models in generative tasks. Here, we illustrate how the alignment methods discussed for diffusion models can be readily adapted for masked language models.

Suppose we aim to decode from x_T (fully masked) to x_0 (non-masked), where each x belongs to the space with size $|K|^L$, with K as the vocabulary size and L as the token length. For x_t ($t \in [0, T]$), several tokens remain masked. Drawing an analogy from diffusion models, we now explain the formulation of the pre-trained policy and value function in masked language models.

- **Pre-Trained Denoising Policy:** Suppose we are now at x_t . At this point, we need to decide which position to unmask. We can use any standard method, such as confidence-based selection, random selection, or left-to-right selection (similar to autoregressive models). After selecting the position, we determine the most suitable token using the encoder’s output using top-K-sampling, for example. We refer to this as the pre-trained policy $p_{t-1}^{\text{pre}}(\cdot | x_t)$ mapping from $|K|^L$ to $\Delta(|K|^L)$ in masked language models.
- **Value Function:** Suppose we are now at x_t . In masked language models, we can unmask from x_t to x_0 in a single step. Denoting this as $\hat{x}_0(x_t)$, we define $r(\hat{x}_0(x_t))$ as the value function. This approach is analogous to defining the value function as in the posterior mean approximation, as discussed in [Section 2.2.1](#).

We are now prepared to discuss alignment methods. After defining pre-trained policies and value functions, a natural strategy is to approximate the policy

$$p_{t-1}^*(x_{t-1} | x_t) \propto \exp(r(\hat{x}_0(x_{t-1}))/\alpha) p_{t-1}^{\text{pre}}(x_{t-1} | x_t)$$

to sample from x_{t-1} at the next time step. Any of the previously discussed off-the-shelf strategies, such as SMC-based guidance in [Section 3.1](#) or value-based sampling in [Section 3.2](#), can be applied here.

9 Combining Fine-Tuning with Inference-Time Techniques

While the inference-time techniques discussed so far have proven effective, a potential bottleneck lies in the extended inference time required to generate samples. For instance, in derivative-free guidance ([Section 3](#)), value functions must be evaluated at each time step. Similarly, in derivative-based guidance ([Section 4](#)), the derivatives of value functions need to be computed.

To mitigate this issue, we outline fine-tuning strategies to accelerate inference time. Our primary approach involves *policy distillation*, a widely adopted technique in RL ([Rusu et al., 2015](#); [Czarnecki et al., 2019](#)). We also emphasize its connection to RL-based fine-tuning in diffusion models, which is summarized in [Uehara et al. \(2024\)](#). Finally, we briefly review methods for minimizing inference time in the context of pure diffusion models (i.e., without alignment considerations), which can be applied following policy distillation.

Before delving into the details of policy distillation, we first emphasize the differences between inference-time techniques and standard post-training methods in diffusion models, such as classifier-free fine-tuning and RL-based fine-tuning.

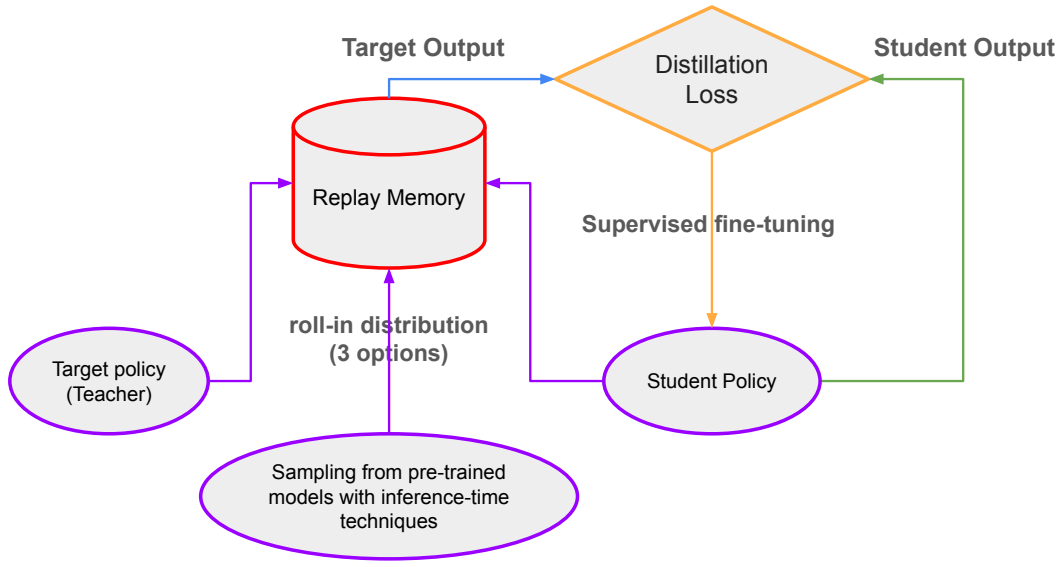


Figure 9: Visualization of policy distillation that leverages inference-time techniques in fine-tuning.

9.1 Comparison with Standard Post-Training Methods

We compare inference-time techniques with several alternative post-training approaches that achieve the same goal—generating natural-like designs with high functionality.

9.1.1 Classifier-Free Fine-Tuning

Classifier-free guidance (Ho and Salimans, 2022) aims to directly model the target conditional distribution $p^{(\alpha)}(x | y)$ by leveraging an unconditional model and adjusting the guidance scale. This method can be applied to fine-tuning when we have a pre-trained model, which characterizes $p^{\text{pre}} \in \Delta(\mathcal{X})$, and a reward (or classifier) as follows:

1. Construct a dataset $\mathcal{D} = \{x_i, y_i\}$ where $x \sim p^{\text{pre}}(x)$ and $y = r(x)$ (or $y \sim p(y | x)$). If an alternative dataset \mathcal{D}' is available, it can be used to augment the dataset.
2. Perform classifier-free guidance by fine-tuning the pre-trained model with the constructed dataset. Here, we augment the model with additional parameters to integrate new conditioning y , as implemented in ControlNet (Zhang et al., 2023).
3. After fine-tuning, if the objective is conditioning, generate samples conditioned on the target y . If the objective is alignment, condition on high values of y .

The performance of this approach is highly dependent on the amount of data available in the first step. Specifically, when working with known reward feedback (e.g., inverse problems or non-differentiable simulation-based feedback), this method can be extremely sample-inefficient, as the feedback must be translated into a large dataset that effectively captures the reward signal.

Furthermore, this dataset must be transformed into models with additional parameters, which significantly increases computational requirements during both training and inference.

Furthermore, this sample inefficiency becomes more severe when the pre-trained models are conditional diffusion models $p(x | c) : \mathcal{C} \rightarrow \Delta(\mathcal{X})$, and multiple classifiers or rewards $r_1 : \mathcal{X} \rightarrow \mathbb{R}, \dots, r_M : \mathcal{X} \rightarrow \mathbb{R}$ need to be optimized. In such cases, it is necessary to construct pairs of the form $\{c, x, r_1(x), \dots, r_M(x)\}$, rather than separate datasets $\{x, r_i(x)\}$ for each reward function, which requires considerable effort. By contrast, the inference-time techniques reviewed in this work do not involve inefficient data augmentation steps or potentially challenging training processes.

Finally, it is worth noting that the inference-time techniques introduced so far could assist in classifier-free fine-tuning during the data augmentation step. In this way, classifier-free fine-tuning and inference-time techniques can be integrated in a complementary manner.

9.1.2 RL-Based Fine-Tuning

RL-based fine-tuning has been employed to optimize rewards by embedding diffusion models into Markov Decision Processes (MDPs). Seminal works have been proposed using policy gradient methods such as PPO (Fan et al., 2023; Black et al., 2023). However, given that many important reward functions in computer vision are differentiable, recent state-of-the-art methods focus on variants of direct backpropagation approaches (Clark et al., 2023; Prabhudesai et al., 2023).

In molecular design, RL-based fine-tuning presents additional challenges, as most useful feedback is highly non-differentiable. In many cases, policy gradient methods remain necessary over direct backpropagation. However, based on the authors’ experience, optimizing such reward functions through policy gradient-based fine-tuning is still difficult, as the landscapes of reward functions are highly complicated.

In contrast, the inference-time techniques introduced in this review are straightforward to implement, as many of them are not only fine-tuning-free but also training-free. As will be discussed in Section 2, while both RL-based and inference-time methods ideally aim to reach the same optimal policy, inference-time techniques are generally more stable for alignment. This is because they directly sample from the optimal target policy by guiding individual particles (samples) without altering the underlying diffusion models. On the other hand, RL-based fine-tuning must guide the entire generative model, which encapsulates the information of all generated samples. As a result, RL-based fine-tuning is significantly more challenging. Consequently, inference-time techniques are more effective across various domains, including molecular design, even when reward feedback is highly non-differentiable, as demonstrated in Li et al. (2024).

Lastly, we highlight that inference-time methods can also enhance fine-tuning through policy distillation. We compare this hybrid approach with RL-based fine-tuning in more detail in Section 9.

9.2 Policy Distillation

So far, we have discussed two standard techniques for post-training. In this subsection, we introduce an alternative approach: policy distillation for fine-tuning, leveraging the inference-time techniques presented earlier. The key idea is to fine-tune diffusion models so that the fine-tuned models replicate the trajectories generated by the inference-time technique. Through the iterative application of this process, the fine-tuned models can gradually improve, as illustrated in Figure 9.

Hereafter, we refer to the inference-time techniques (e.g., SMC-based guidance, value-based importance sampling, and classifier guidance targeting $p_{t-1}^* : \mathcal{X} \rightarrow \Delta(\mathcal{X})$) as teacher policies. The policies being fine-tuned, represented as $p_{t-1}(\cdot | \cdot; \theta) : \mathcal{X} \rightarrow \Delta(\mathcal{X})$, are referred to as student policies, adopting the terminology from RL (Czarnecki et al., 2019).

Algorithms in this section are summarized in the following master formulation.

Master Formulation

Introducing a roll-in distribution $u_t \in \Delta(\mathcal{X})$, and an f -divergence between teacher and student policies at time t , the policy distillation is formulated as an iterative algorithm using the update:

$$\theta^{\text{new}} \leftarrow \theta^{\text{old}} - \gamma \sum_{t=T+1}^1 \mathbb{E}_{x_t \sim u_t} [\nabla_{\theta} f(p_{t-1}^*(\cdot | x_t) \| p_{t-1}(\cdot | x_t; \theta))] |_{\theta^{\text{old}}},$$

where γ is a learning rate.

Hereafter, we elaborate on two critical points.

9.2.1 Choice of Roll-In Distributions

The selection of the roll-in distribution is critical, as optimizing the empirical objective with function approximation ensures low error only within the distribution’s support. Potential choices include (1) the teacher policy, (2) the student policy (the one being optimized), and (3) data recycling via forward processes. These distributions can also be mixed. We will explore these options in greater detail.

Teacher Policy. This approach is often called offline policy distillation, as the roll-in distribution remains fixed throughout fine-tuning. Since this corresponds to the target policy, it is always a reasonable choice. However, it could have a distributional shift (Ross and Bagnell, 2010): during fine-tuning, the model encounters states it has not previously observed yet, which can result in poor performance.

Student Policy. This approach is often referred to as online policy distillation, as roll-in samples are collected in an online manner. In the RL context, it is employed in the well-known algorithm DAgger (Ross et al., 2011). This method mitigates the distributional shift issue mentioned earlier by aligning the training distribution with the distribution induced by the current student policy. In practice, it can be beneficial to mix distributions induced by both teacher and student policies, as demonstrated in Ross et al. (2011); Sun et al. (2017); Chang et al. (2023).

Data Recycling via Forward Processes. In both scenarios described above (using teacher or student policies as roll-in distributions), the roll-in distributions are generated by sampling from x_T to x_t . However, employing teacher policies as roll-in distributions can be computationally expensive.

To mitigate this inefficiency, an alternative approach leverages the forward process in pre-trained diffusion models, sampling from x_0 to x_t , which is computationally faster than sampling from x_T to x_t . Specifically, assume we have access to the dataset used to train the pre-trained models or data obtained at time 0 through inference-time techniques. Let this dataset be denoted as $\mathcal{D} = \{x_0^i\}_{i=1}^N$. Using this dataset \mathcal{D} , we can generate roll-in distributions by sampling x_t from the forward policies of the pre-trained models, starting from x_0 . Consequently, the loss function becomes:

$$\frac{1}{|\mathcal{D}|} \sum_{i=1}^{|\mathcal{D}|} \sum_{t=T+1}^1 \mathbb{E}_{x_t \sim q_t(\cdot | x_0^i)} [f(p_{t-1}^*(\cdot | x_t) \| p_{t-1}(\cdot | x_t; \theta))], \quad (22)$$

where $q_t(\cdot | x_0^i)$ represents the distribution induced by the forward policies of the pre-trained models from x_0 to x_t .

9.2.2 Choice of Divergence

The choice of divergence is critical. Common options include KL divergence and inverse KL divergence.

KL Divergence. In this case, the gradient is

$$\sum_{t=T+1}^1 \mathbb{E}_{x_t \sim u_t} [\nabla_{\theta} \text{KL}(p_{t-1}^*(\cdot | x_t) \| p_{t-1}(\cdot | x_t; \theta))] |_{\theta^{\text{old}}}. \quad (23)$$

This can be further simplified to:

$$\sum_{t=T+1}^1 \mathbb{E}_{x_t \sim u_t, x_{t-1} \sim p^*(x_t)} [\nabla_{\theta} \log p_{t-1}(x_{t-1} | x_t; \theta)] |_{\theta^{\text{old}}}.$$

When using marginal distributions induced by teacher policies as roll-in distributions, this approach is particularly intuitive, as it minimizes the KL divergence between the distributions induced by the teacher and student policies. In generative models, KL divergence is commonly employed since it effectively covers the target distribution (i.e., it is less mode-seeking but more conservative).

Inverse KL Divergence. In this case, the gradient is

$$\sum_{t=T+1}^1 \mathbb{E}_{x_t \sim u_t} [\nabla_{\theta} \text{KL}(p_{t-1}(\cdot | x_t; \theta) \| p_{t-1}^*(\cdot | x_t))] |_{\theta^{\text{old}}}. \quad (24)$$

Substituting the form of the optimal policy p_{t-1}^* , it simplifies to:

$$\sum_{t=T}^0 \mathbb{E}_{x_t \sim u_t} \left[\nabla_{\theta} \mathbb{E}_{x_{t-1} \sim p_{t-1}(x_t; \theta)} \left[\log p_{t-1}(x_{t-1} | x_t; \theta) - \log p_{t-1}^{\text{pre}}(x_{t-1} | x_t) - \frac{v_{t-1}(x_{t-1})}{\alpha} + \frac{v_t(x_t)}{\alpha} \Big| x_t \right] \right]. \quad (25)$$

This method is inherently more mode-seeking. While this property can be disadvantageous when the goal is to cover diverse regions, it becomes beneficial when the primary focus is on optimization without prioritizing diversity.

9.3 Relation to RL-Based Fine-Tuning

In this section, we establish the connection between the policy distillation approach discussed earlier and existing RL-based fine-tuning methods, which are summarized in [Uehara et al. \(2024\)](#).

9.3.1 Value-Weighted MLE (Reward-Weighted MLE)

First, we relate the KL-based distillation approach to value-weighted maximum likelihood estimation (MLE). Recall that p_{t-1}^* is a value-tilted policy proportional to $p_{t-1}^{\text{pre}}(\cdot | x_{t-1}) \exp(v_{t-1}(\cdot))$. When the divergence function f is the KL divergence, the gradient formulation (23) becomes:

$$\sum_{t=T+1}^1 \mathbb{E}_{x_t \sim u_t} \left[\nabla_{\theta} \mathbb{E}_{x_{t-1} \sim p^{\text{pre}}(x_t)} \left[\exp \left(\frac{v_{t-1}(x_{t-1})}{\alpha} \right) \log p_{t-1}(x_{t-1} | x_t; \theta) \right] \right].$$

This formulation is known in the RL literature as value-weighted MLE ([Peng et al., 2019](#); [Peters et al., 2010](#)). In the context of fine-tuning diffusion models, it reduces to the objective function defined in [Uehara et al. \(2024, Algorithm 3\)](#).

9.3.2 Path Consistency Learning (loss used in Gflownets)

Next, recall the soft-Bellman equation:

$$\int p_{t-1}^{\text{pre}}(x | x_t) \exp(v_{t-1}(x)/\alpha) dx = \exp(v_t(x_t)/\alpha).$$

Then, by taking the logarithm of the optimal policy

$$p_{t-1}^{\text{pre}}(\cdot | x_t) = \exp(v_{t-1}(\cdot)/\alpha) p_{t-1}^{\text{pre}}(x | x_t) / \exp(v_t(x_t)/\alpha),$$

this reduces to

$$\log p_{t-1}^*(x_{t-1} | x_t) - \log p_{t-1}^{\text{pre}}(x_{t-1} | x_t) - \frac{v_{t-1}(x_{t-1})}{\alpha} + \frac{v_t(x_t)}{\alpha} = 0.$$

From the above equation, the optimal policy is estimated by minimizing the following objective:

$$\sum_{t=T+1}^1 \mathbb{E}_{(x_{t-1}, x_t) \sim u_t} \left[\left\| \log p_{t-1}(x_{t-1} | x_t; \theta) - \log p_{t-1}^{\text{pre}}(x_{t-1} | x_t) - \frac{v_{t-1}(x_{t-1})}{\alpha} + \frac{v_t(x_t)}{\alpha} \right\|^2 \right].$$

This objective aligns with the path-consistency RL objective commonly discussed in the RL literature ([Nachum et al., 2017](#)). In RL-based fine-tuning, it reduces to the objective defined in [Uehara et al. \(2024, Algorithm 5\)](#). Note several improved variants have also been proposed in [Rector-Brooks et al. \(2024\)](#); [Venkatraman et al. \(2024\)](#).

The above is closely related to the inverse KL divergence objective (25). However, PCL is generally regarded as more stable, as the expectation in (25) depends on the parameter being optimized.

9.3.3 PPO and Direct Backpropagation

In the RL-based fine-tuning literature (Fan et al., 2023; Black et al., 2023), the standard objective is:

$$\operatorname{argmax}_{\theta} \mathbb{E}_{\{p_t^\theta\}_{t=T+1}^1} \left[r(x_0) - \alpha \sum_{t=T+1}^1 \operatorname{KL}(p_{t-1}(\cdot | x_t; \theta) \| p_{t-1}^{\text{pre}}(\cdot | x_t)) \right], \quad (26)$$

where the expectation is taken with respect to p^θ . As demonstrated in Uehara et al. (2024, Theorem 1), the policy that maximizes the above (in the absence of optimization or function approximation errors) is equal to the optimal policy we aim to target during inference, i.e., p_{t-1}^* in (8).

While solving the optimization problem in (26) is non-trivial in practice, policy gradient methods (or their variants) can be employed (Black et al., 2023; Fan et al., 2023). Then, ignoring KL terms to simplify the notation here, the optimization step becomes

$$\theta^{\text{old}} + \gamma \mathbb{E}_{\{p_t^{\theta^{\text{old}}}\}_{t=T+1}^1} \left[r(x_0) \sum_{t=T+1}^1 \frac{\nabla_{\theta} p_{t-1}(\cdot | x_t; \theta)}{p_{t-1}(\cdot | x_t; \theta^{\text{old}})} \right]_{\theta^{\text{old}}}. \quad (27)$$

Furthermore, when the reward function is differentiable, direct backpropagation becomes a feasible approach (Clark et al., 2023; Prabhudesai et al., 2023).

It is worthwhile to note the above objective function in (26) is essentially equivalent to the inverse KL divergence:

$$\sum_{t=T+1}^1 \mathbb{E}_{\{p_t^\theta\}_{t=T+1}^1} [\operatorname{KL}(p_{t-1}(\cdot | x_{t-1}; \theta) \| p_{t-1}^*(\cdot | x_{t-1}))].$$

This is seen by

$$\begin{aligned} & -\alpha \sum_{t=T+1}^1 \mathbb{E}_{\{p_t^\theta\}_{t=T+1}^1} [\operatorname{KL}(p_{t-1}(\cdot | x_{t-1}; \theta) \| p_{t-1}^*(\cdot | x_{t-1}))] \\ &= -\alpha \sum_{t=T+1}^1 \mathbb{E}_{\{p_t^\theta\}_{t=T+1}^1} [\log p_{t-1}(x_{t-1} | x_t; \theta) - \log p_{t-1}^{\text{pre}}(x_{t-1} | x_t) - v_{t-1}(x_{t-1}) + v_t(x_t)] \\ &= \mathbb{E}_{\{p_t^\theta\}_{t=T+1}^1} \left[r(x_0) - \alpha \sum_{t=T+1}^1 \operatorname{KL}(p_{t-1}(\cdot | x_t; \theta) \| p_{t-1}^{\text{pre}}(\cdot | x_t)) \right]. \end{aligned}$$

Thus, RL-based fine-tuning is considered to be similar to the policy distillation approach using the inverse KL divergence.

However, the distillation approach using inverse KL, as discussed in (24), uses the estimation of value functions, leading to substantially different practical behavior, while the PPO/direct backpropagation approaches do not estimate value functions explicitly.

9.4 Differences between Policy Distillation and RL-Based Fine-Tuning

Here, we briefly compare two approaches: policy distillation and RL-based fine-tuning. For clarity, by policy distillation, we refer to the simplest KL-based approach in (23), and by RL-based fine-tuning, we refer to the PPO approach (Black et al., 2023; Fan et al., 2023), which optimizes the objective function in (26) with PPO (Schulman et al., 2017).

Advantages of Policy Distillation over PPO. The primary advantage lies in the stability of the fine-tuning process. Policy distillation using KL divergence is equivalent to supervised learning toward target optimal policies, ensuring stable fine-tuning since the target remains fixed. Additionally, policy distillation can function as an offline algorithm, with roll-in distributions independent of current policies (student policies) and could be technically any roll-in distributions.

In contrast, PPO introduces instability due to the need for continuously updating roll-in distributions and optimizing a dynamic objective function involving ratios relative to the evolving policies being trained. Although PPO incorporates conservative updates with KL constraints (as seen in TRPO (Schulman et al., 2015) and CPI (Kakade and Langford, 2002)) to mitigate this instability, ensuring stable updates remains challenging in practice, often resulting in convergence to suboptimal local minima before reaching optimal policies. Furthermore, while related methods, such as direct backpropagation (Clark et al., 2023; Prabhudesai et al., 2023), can address some of these optimization challenges, they require differentiable models, which are difficult to construct in molecular design.

A second advantage is policy distillation’s robustness against reward over-optimization. This issue arises when generative models over-exploit learned reward functions, resulting in out-of-distribution samples that achieve low genuine rewards. Policy distillation inherently avoids this issue since roll-in samples are generated using inference-time techniques, i.e., essentially modified pre-trained models, that are more likely to stay on the manifold, reflecting natural-like designs (e.g., natural image spaces in computer vision or chemical/biological spaces in molecular design).

In contrast, PPO’s dynamic roll-in distributions can easily deviate from these natural manifolds. Although techniques such as KL penalization against deviations from pre-trained policies, as outlined in (26), and the use of conservative reward models (Uehara et al., 2024) can help mitigate this issue, the non-conservative nature of the approach may still pose challenges.

9.5 Further Extensions with “Distillation”

After distilling optimal policies, we can apply additional standard “distillation” techniques in diffusion models. Notably, unlike policy distillation, the typical objective of these “distillation” methods is to reduce inference time while preserving the naturalness of the generated samples, without involving reward maximization.

Distillation. The focus of distillation in diffusion models is to reduce the number of discretization steps while maintaining the quality of the generated samples (Salimans and Ho, 2022; Sun et al., 2023; Meng et al., 2023). For example, a widely adopted approach is progressive distillation (Salimans and Ho, 2022), which iteratively halves the number of discretization steps with each stage of the distillation process.

Consistency Distillation/Training. Consistency training aims to ensure that the model’s predictions remain stable across multiple timesteps during the reverse diffusion process. The primary motivation is to minimize the number of reverse steps required without compromising the quality of the generated samples. For further details, refer to Song et al. (2023); Li et al. (2024); Ding and Jin (2023).

10 More Related Works

We have covered various aspects of inference-time techniques in diffusion models. In this section, we finally outline additional related topics that were not the primary focus of our discussion.

10.1 Walk-Jump Sampling for Protein Design

Walk-Jump Sampling (Frey et al., 2023; Saremi and Hyvärinen, 2019) is an algorithm designed to achieve high reward values while preserving the naturalness of the generated designs, making it particularly effective for antibody design.

The intuition behind walk-jump sampling can be summarized as follows. Similar to our objective in Section 1.2, the goal is to sample from the distribution $\exp(r(x))/\alpha p^{\text{pre}}(x)$. One approach to achieve this is through Langevin Monte Carlo (LMC), also known as the Metropolis-adjusted Langevin algorithm (MALA): sampling using the following update:

$$y_k \leftarrow y_{k-1} + \beta \{ \nabla r(y_{k-1})/\alpha + \nabla_x \log p^{\text{pre}}(x)|_{y_{k-1}} \} + \sqrt{2\beta} \epsilon_k, \quad \epsilon_k \sim \mathcal{N}(0, 1). \quad (28)$$

However, the score function $\nabla_x \log p^{\text{pre}}(x)$ is unknown. A common method for estimating the score is through denoising score matching (Vincent, 2011):

$$\hat{\theta} = \underset{\theta}{\operatorname{argmin}} \mathbb{E}_{x \sim p^{\text{pre}}, \tilde{x} \sim \mathcal{N}(x, \sigma^2 I)} \left[\left\| \frac{x - \tilde{x}}{\sigma^2} - s(\tilde{x}; \theta) \right\|^2 \right].$$

By plugging this into (28), the LMC algorithm is an iterative algorithm using the following update:

$$y_k \leftarrow y_{k-1} + \beta \left\{ \underbrace{\nabla r(y_{k-1})/\alpha}_{\text{Walk}} + \underbrace{s(y_{k-1}; \hat{\theta})}_{\text{Jump}} \right\} + \sqrt{2\beta} \epsilon_k. \quad (29)$$

Building on this intuition, walk-in jump sampling is defined as an algorithm that iteratively performs a “walk” (adding the gradient of the reward) followed by a “jump” (adding a score) as described above.

Importantly, walk-in jump sampling can be viewed as a variant of classifier guidance, where a single noise level is employed, as follows. For this purpose, recall that while the diffusion model can be framed in terms of variational inference (Ho et al., 2020) or time-reversal SDEs (Song et al., 2021), another popular derivation involves running MALA with score function estimation at multiple noise levels, known as score-based models (SBMs) (Song and Ermon, 2019). Thus, walk-jump sampling is similar to classifier guidance explained in Section 4 where only a single noise level is used. However, the key difference is that the score and gradient are iteratively updated in an MCMC framework, rather than progressing sequentially from $t = T$ to $t = 0$, as in classifier guidance. For further details, please refer to the original papers.

10.2 Hallucination Approaches for Protein Design

The term “hallucination” (or its variants) frequently refers to sequential refinement methods in silico protein design. Specifically, this algorithm iteratively refines a sequence based on predefined reward functions. Standard methods for sequence refinement include MCMC (Anishchenko et al.,

2021), evolutionary algorithms (Jendrusch et al., 2021), and gradient-based algorithms (Goverde et al., 2023; Jeliaskov et al., 2023). In our context, Section 7 is closely related. Common reward functions include the loss between the predicted structure (using structural prediction models such as AlphaFold or ESMFold (Ahdritz et al., 2024)) and the target structure, as well as metrics like stability, binding activity, and geometric constraints.

10.3 Inference-Time Techniques for Inpainting and Linear Inverse Problems.

Inpainting tasks involve reconstructing or filling in missing or corrupted regions of an image in a manner that appears natural and consistent with the surrounding content. In the context of protein design, a similar challenge is known as motif scaffolding, as mentioned in the introduction. For inpainting tasks, replacement methods (e.g., Song et al. (2021)) are commonly employed. These approaches map the conditioned region (known location) through the forward process and replace it with generated samples at each step of the inference process. While this method is somewhat heuristic, a more refined version incorporating SMC was later proposed by Trippe et al. (2022), demonstrating success in motif scaffolding.

Additionally, for related tasks like linear inverse problems, more specialized algorithms have recently been introduced (Song et al., 2023; Chung et al., 2022; Kawar et al., 2022). Although these methods may not be as broadly applicable as those discussed here, they offer superior performance in specific, constrained scenarios.

10.4 Speculative Decoding.

Speculative decoding is an inference-time technique used in NLP to accelerate the generation process (Leviathan et al., 2023). The key idea is to generate multiple candidate tokens simultaneously using a smaller, faster model and validate them with a larger, more powerful model. As models grow larger in protein design, adopting similar techniques could offer substantial benefits in accelerating inference in this field as well.

Acknowledgement

The authors would like to thank Amy Wang, Francisco Vargas, Christian A. Naesseth for valuable discussions and feedback.

References

- Abramson, J., J. Adler, J. Dunger, R. Evans, T. Green, A. Pritzel, O. Ronneberger, L. Willmore, A. J. Ballard, J. Bambrick, et al. (2024). Accurate structure prediction of biomolecular interactions with alphafold 3. *Nature*, 1–3.
- Ahdritz, G., N. Bouatta, C. Floristean, S. Kadyan, Q. Xia, W. Gerecke, T. J. O’Donnell, D. Berenberg, I. Fisk, N. Zanichelli, et al. (2024). Openfold: Retraining alphafold2 yields new insights into its learning mechanisms and capacity for generalization. *Nature Methods*, 1–11.

- Akiyama, M. and Y. Sakakibara (2022). Informative rna base embedding for rna structural alignment and clustering by deep representation learning. *NAR genomics and bioinformatics* 4(1), lqac012.
- Alamdari, S., N. Thakkar, R. van den Berg, A. X. Lu, N. Fusi, A. P. Amini, and K. K. Yang (2023). Protein generation with evolutionary diffusion: sequence is all you need. *bioRxiv*, 2023–09.
- Anderson, B. D. (1982). Reverse-time diffusion equation models. *Stochastic Processes and their Applications* 12(3), 313–326.
- Anishchenko, I., S. J. Pellock, T. M. Chidyausiku, T. A. Ramelot, S. Ovchinnikov, J. Hao, K. Bafna, C. Norn, A. Kang, A. K. Bera, et al. (2021). De novo protein design by deep network hallucination. *Nature* 600(7889), 547–552.
- Austin, J., D. D. Johnson, J. Ho, D. Tarlow, and R. Van Den Berg (2021). Structured denoising diffusion models in discrete state-spaces. *Advances in Neural Information Processing Systems* 34, 17981–17993.
- Bachas, S., G. Rakocevic, D. Spencer, A. V. Sastry, R. Haile, J. M. Sutton, G. Kasun, A. Stachyra, J. M. Gutierrez, E. Yassine, et al. (2022). Antibody optimization enabled by artificial intelligence predictions of binding affinity and naturalness. *BioRxiv*, 2022–08.
- Bansal, A., H.-M. Chu, A. Schwarzschild, S. Sengupta, M. Goldblum, J. Geiping, and T. Goldstein (2023). Universal guidance for diffusion models. In *Proceedings of the IEEE/CVF Conference on Computer Vision and Pattern Recognition*, pp. 843–852.
- Bengio, Y., S. Lahlou, T. Deleu, E. J. Hu, M. Tiwari, and E. Bengio (2023). Gflownet foundations. *Journal of Machine Learning Research* 24(210), 1–55.
- Black, K., M. Janner, Y. Du, I. Kostrikov, and S. Levine (2023). Training diffusion models with reinforcement learning. *arXiv preprint arXiv:2305.13301*.
- Branke, J. (2008). *Multiobjective optimization: Interactive and evolutionary approaches*, Volume 5252. Springer Science & Business Media.
- Brown, T. B. (2020). Language models are few-shot learners. *arXiv preprint arXiv:2005.14165*.
- Campbell, A., J. Benton, V. De Bortoli, T. Rainforth, G. Deligiannidis, and A. Doucet (2022). A continuous time framework for discrete denoising models. *Advances in Neural Information Processing Systems* 35, 28266–28279.
- Campbell, A., J. Yim, R. Barzilay, T. Rainforth, and T. Jaakkola (2024). Generative flows on discrete state-spaces: Enabling multimodal flows with applications to protein co-design. *arXiv preprint arXiv:2402.04997*.
- Cardoso, G., Y. J. E. Idrissi, S. L. Corff, and E. Moulines (2023). Monte carlo guided diffusion for bayesian linear inverse problems. *arXiv preprint arXiv:2308.07983*.
- Chang, J. D., K. Brantley, R. Ramamurthy, D. Misra, and W. Sun (2023). Learning to generate better than your llm. *arXiv preprint arXiv:2306.11816*.

- Chaudhury, S., S. Lyskov, and J. J. Gray (2010). Pyrosetta: a script-based interface for implementing molecular modeling algorithms using rosetta. *Bioinformatics* 26(5), 689–691.
- Chen, R. T. and Y. Lipman (2023). Riemannian flow matching on general geometries. *arXiv preprint arXiv:2302.03660*.
- Chetrite, R. and H. Touchette (2015). Nonequilibrium markov processes conditioned on large deviations. In *Annales Henri Poincaré*, Volume 16, pp. 2005–2057. Springer.
- Chu, A. E., J. Kim, L. Cheng, G. El Nesr, M. Xu, R. W. Shuai, and P.-S. Huang (2024). An all-atom protein generative model. *Proceedings of the National Academy of Sciences* 121(27), e2311500121.
- Chung, H., J. Kim, M. T. Mccann, M. L. Klasky, and J. C. Ye (2022). Diffusion posterior sampling for general noisy inverse problems. *arXiv preprint arXiv:2209.14687*.
- Chung, H., B. Sim, D. Ryu, and J. C. Ye (2022). Improving diffusion models for inverse problems using manifold constraints. *Advances in Neural Information Processing Systems* 35, 25683–25696.
- Clark, K., P. Vicol, K. Swersky, and D. J. Fleet (2023). Directly fine-tuning diffusion models on differentiable rewards. *arXiv preprint arXiv:2309.17400*.
- Corso, G., H. Stärk, B. Jing, R. Barzilay, and T. Jaakkola (2022). Diffdock: Diffusion steps, twists, and turns for molecular docking. *arXiv preprint arXiv:2210.01776*.
- Cretu, M., C. Harris, J. Roy, E. Bengio, and P. Liò (2024). Synflownet: Towards molecule design with guaranteed synthesis pathways. In *ICLR 2024 Workshop on Generative and Experimental Perspectives for Biomolecular Design*.
- Czarnecki, W. M., R. Pascanu, S. Osindero, S. Jayakumar, G. Swirszcz, and M. Jaderberg (2019). Distilling policy distillation. In *The 22nd international conference on artificial intelligence and statistics*, pp. 1331–1340. PMLR.
- Dathathri, S., A. Madotto, J. Lan, J. Hung, E. Frank, P. Molino, J. Yosinski, and R. Liu (2019). Plug and play language models: A simple approach to controlled text generation. *arXiv preprint arXiv:1912.02164*.
- Dauparas, J., I. Anishchenko, N. Bennett, H. Bai, R. J. Ragotte, L. F. Milles, B. I. Wicky, A. Courbet, R. J. de Haas, N. Bethel, et al. (2022). Robust deep learning–based protein sequence design using proteinmpnn. *Science* 378(6615), 49–56.
- De Bortoli, V., E. Mathieu, M. Hutchinson, J. Thornton, Y. W. Teh, and A. Doucet (2022). Riemannian score-based generative modelling. *Advances in Neural Information Processing Systems* 35, 2406–2422.
- Del Moral, P., A. Doucet, and A. Jasra (2006). Sequential monte carlo samplers. *Journal of the Royal Statistical Society Series B: Statistical Methodology* 68(3), 411–436.

- Deng, H. and C. Raffel (2023). Reward-augmented decoding: Efficient controlled text generation with a unidirectional reward model. *arXiv preprint arXiv:2310.09520*.
- Denker, A., F. Vargas, S. Padhy, K. Didi, S. V. Mathis, R. Barbano, V. Dutordoir, E. Mathieu, U. J. Komorowska, and P. Lio (2024). Deft: Efficient fine-tuning of diffusion models by learning the generalised h -transform. In *The Thirty-eighth Annual Conference on Neural Information Processing Systems*.
- Devlin, J. (2018). Bert: Pre-training of deep bidirectional transformers for language understanding. *arXiv preprint arXiv:1810.04805*.
- Dhariwal, P. and A. Nichol (2021). Diffusion models beat gans on image synthesis. *Advances in neural information processing systems 34*, 8780–8794.
- Ding, Z. and C. Jin (2023). Consistency models as a rich and efficient policy class for reinforcement learning. *arXiv preprint arXiv:2309.16984*.
- Dou, Z. and Y. Song (2024). Diffusion posterior sampling for linear inverse problem solving: A filtering perspective. In *The Twelfth International Conference on Learning Representations*.
- Doucet, A., A. M. Johansen, et al. (2009). A tutorial on particle filtering and smoothing: Fifteen years later. *Handbook of nonlinear filtering 12*(656-704), 3.
- Ernst, D., P. Geurts, and L. Wehenkel (2005). Tree-based batch mode reinforcement learning. *Journal of Machine Learning Research 6*.
- Fan, Y., O. Watkins, Y. Du, H. Liu, M. Ryu, C. Boutilier, P. Abbeel, M. Ghavamzadeh, K. Lee, and K. Lee (2023). DPOK: Reinforcement learning for fine-tuning text-to-image diffusion models. *arXiv preprint arXiv:2305.16381*.
- Feng, X., Z. Wan, M. Wen, S. M. McAleer, Y. Wen, W. Zhang, and J. Wang (2023). Alphazero-like tree-search can guide large language model decoding and training. *arXiv preprint arXiv:2309.17179*.
- Frey, N. C., D. Berenberg, K. Zadorozhny, J. Kleinhenz, J. Lafrance-Vanasse, I. Hotzel, Y. Wu, S. Ra, R. Bonneau, K. Cho, et al. (2023). Protein discovery with discrete walk-jump sampling. *arXiv preprint arXiv:2306.12360*.
- Geist, M., B. Scherrer, and O. Pietquin (2019). A theory of regularized markov decision processes. In *International Conference on Machine Learning*, pp. 2160–2169. PMLR.
- Gordon, N. J., D. J. Salmond, and A. F. Smith (1993). Novel approach to nonlinear/non-gaussian bayesian state estimation. In *IEE proceedings F (radar and signal processing)*, Volume 140, pp. 107–113. IET.
- Goverde, C. A., B. Wolf, H. Khakzad, S. Rosset, and B. E. Correia (2023). De novo protein design by inversion of the alphafold structure prediction network. *Protein Science 32*(6), e4653.

- Grill, J.-B., F. Altché, Y. Tang, T. Hubert, M. Valko, I. Antonoglou, and R. Munos (2020). Monte-carlo tree search as regularized policy optimization. In *International Conference on Machine Learning*, pp. 3769–3778. PMLR.
- Haarnoja, T., H. Tang, P. Abbeel, and S. Levine (2017). Reinforcement learning with deep energy-based policies. In *International conference on machine learning*, pp. 1352–1361. PMLR.
- Halgren, T. A., R. B. Murphy, R. A. Friesner, H. S. Beard, L. L. Frye, W. T. Pollard, and J. L. Banks (2004). Glide: a new approach for rapid, accurate docking and scoring. 2. enrichment factors in database screening. *Journal of medicinal chemistry* 47(7), 1750–1759.
- Han, S., I. Shenfeld, A. Srivastava, Y. Kim, and P. Agrawal (2024). Value augmented sampling for language model alignment and personalization. *arXiv preprint arXiv:2405.06639*.
- Hao, S., Y. Gu, H. Ma, J. J. Hong, Z. Wang, D. Z. Wang, and Z. Hu (2023). Reasoning with language model is planning with world model. *arXiv preprint arXiv:2305.14992*.
- Hayes, T., R. Rao, H. Akin, N. J. Sofroniew, D. Oktay, Z. Lin, R. Verkuil, V. Q. Tran, J. Deaton, M. Wiggert, et al. (2024). Simulating 500 million years of evolution with a language model. *bioRxiv*, 2024–07.
- He, K., X. Chen, S. Xie, Y. Li, P. Dollár, and R. Girshick (2022). Masked autoencoders are scalable vision learners. In *Proceedings of the IEEE/CVF conference on computer vision and pattern recognition*, pp. 16000–16009.
- Heng, J., A. N. Bishop, G. Deligiannidis, and A. Doucet (2020). Controlled sequential monte carlo.
- Hie, B., S. Candido, Z. Lin, O. Kabeli, R. Rao, N. Smetanin, T. Sercu, and A. Rives (2022). A high-level programming language for generative protein design. *bioRxiv*, 2022–12.
- Hie, B. L., V. R. Shanker, D. Xu, T. U. Bruun, P. A. Weidenbacher, S. Tang, W. Wu, J. E. Pak, and P. S. Kim (2024). Efficient evolution of human antibodies from general protein language models. *Nature Biotechnology* 42(2), 275–283.
- Ho, J., A. Jain, and P. Abbeel (2020). Denoising diffusion probabilistic models. *Advances in neural information processing systems* 33, 6840–6851.
- Ho, J. and T. Salimans (2022). Classifier-free diffusion guidance. *arXiv preprint arXiv:2207.12598*.
- Ho, J., T. Salimans, A. Gritsenko, W. Chan, M. Norouzi, and D. J. Fleet (2022). Video diffusion models. *Advances in Neural Information Processing Systems* 35, 8633–8646.
- Hubert, T., J. Schrittwieser, I. Antonoglou, M. Barekatin, S. Schmitt, and D. Silver (2021). Learning and planning in complex action spaces. In *International Conference on Machine Learning*, pp. 4476–4486. PMLR.
- Hyvärinen, A. (2007). Some extensions of score matching. *Computational statistics & data analysis* 51(5), 2499–2512.

- Hyvärinen, A. and P. Dayan (2005). Estimation of non-normalized statistical models by score matching. *Journal of Machine Learning Research* 6(4).
- Ingraham, J. B., M. Baranov, Z. Costello, K. W. Barber, W. Wang, A. Ismail, V. Frappier, D. M. Lord, C. Ng-Thow-Hing, E. R. Van Vlack, et al. (2023). Illuminating protein space with a programmable generative model. *Nature* 623(7989), 1070–1078.
- Jeliazkov, J. R., D. del Alamo, and J. D. Karpiak (2023). Esmfold hallucinates native-like protein sequences. *bioRxiv*, 2023–05.
- Jendrusch, M., J. O. Korbel, and S. K. Sadiq (2021). Alphadesign: A de novo protein design framework based on alphafold. *Biorxiv*, 2021–10.
- Ji, Y., Z. Zhou, H. Liu, and R. V. Davuluri (2021). Dnabert: pre-trained bidirectional encoder representations from transformers model for dna-language in genome. *Bioinformatics* 37(15), 2112–2120.
- Jing, B., G. Corso, J. Chang, R. Barzilay, and T. Jaakkola (2022). Torsional diffusion for molecular conformer generation. *Advances in Neural Information Processing Systems* 35, 24240–24253.
- Kajita, S., T. Kinjo, and T. Nishi (2020). Autonomous molecular design by monte-carlo tree search and rapid evaluations using molecular dynamics simulations. *Communications Physics* 3(1), 77.
- Kakade, S. and J. Langford (2002). Approximately optimal approximate reinforcement learning. In *Proceedings of the Nineteenth International Conference on Machine Learning*, pp. 267–274.
- Kawar, B., M. Elad, S. Ermon, and J. Song (2022). Denoising diffusion restoration models. *Advances in Neural Information Processing Systems* 35, 23593–23606.
- Kenton, J. D. M.-W. C. and L. K. Toutanova (2019). Bert: Pre-training of deep bidirectional transformers for language understanding. In *Proceedings of naacL-HLT*, Volume 1, pp. 2. Minneapolis, Minnesota.
- Khanov, M., J. Burapachep, and Y. Li (2024). Args: Alignment as reward-guided search. *arXiv preprint arXiv:2402.01694*.
- Kitagawa, G. (1993). A monte carlo filtering and smoothing method for non-gaussian nonlinear state space models. In *Proceedings of the 2nd US-Japan joint seminar on statistical time series analysis*, Volume 110.
- Kocsis, L. and C. Szepesvári (2006). Bandit based monte-carlo planning. In *European conference on machine learning*, pp. 282–293. Springer.
- Leblond, R., J.-B. Alayrac, L. Sifre, M. Pislár, J.-B. Lespiau, I. Antonoglou, K. Simonyan, and O. Vinyals (2021). Machine translation decoding beyond beam search. *arXiv preprint arXiv:2104.05336*.
- Lee, J. M. (2018). *Introduction to Riemannian manifolds*, Volume 2. Springer.

- Leviathan, Y., M. Kalman, and Y. Matias (2023). Fast inference from transformers via speculative decoding. In *International Conference on Machine Learning*, pp. 19274–19286. PMLR.
- Levin, D. A. and Y. Peres (2017). *Markov chains and mixing times*, Volume 107. American Mathematical Soc.
- Levine, S. (2018). Reinforcement learning and control as probabilistic inference: Tutorial and review. *arXiv preprint arXiv:1805.00909*.
- Lew, A. K., T. Zhi-Xuan, G. Grand, and V. K. Mansinghka (2023). Sequential monte carlo steering of large language models using probabilistic programs. *arXiv preprint arXiv:2306.03081*.
- Li, G., Z. Huang, and Y. Wei (2024). Towards a mathematical theory for consistency training in diffusion models. *arXiv preprint arXiv:2402.07802*.
- Li, H., K.-S. Leung, M.-H. Wong, and P. J. Ballester (2015). Improving autodock vina using random forest: the growing accuracy of binding affinity prediction by the effective exploitation of larger data sets. *Molecular informatics* 34(2-3), 115–126.
- Li, X., Y. Zhao, C. Wang, G. Scalia, G. Eraslan, S. Nair, T. Biancalani, A. Regev, S. Levine, and M. Uehara (2024). Derivative-free guidance in continuous and discrete diffusion models with soft value-based decoding. *arXiv preprint arXiv:2408.08252*.
- Lisanza, S. L., J. M. Gershon, S. Tipps, L. Arnoldt, S. Hendel, J. N. Sims, X. Li, and D. Baker (2023). Joint generation of protein sequence and structure with rosettafold sequence space diffusion. *bioRxiv*, 2023–05.
- Livesey, B. J. and J. A. Marsh (2023). Advancing variant effect prediction using protein language models. *Nature Genetics* 55(9), 1426–1427.
- Lou, A., C. Meng, and S. Ermon (2023). Discrete diffusion language modeling by estimating the ratios of the data distribution. *arXiv preprint arXiv:2310.16834*.
- Luo, C. (2022). Understanding diffusion models: A unified perspective. *arXiv preprint arXiv:2208.11970*.
- Ma, N., S. Tong, H. Jia, H. Hu, Y.-C. Su, M. Zhang, X. Yang, Y. Li, T. Jaakkola, X. Jia, and S. Xie (2025). Inference-time scaling for diffusion models beyond scaling denoising steps.
- Meng, C., R. Rombach, R. Gao, D. Kingma, S. Ermon, J. Ho, and T. Salimans (2023). On distillation of guided diffusion models. In *Proceedings of the IEEE/CVF Conference on Computer Vision and Pattern Recognition*, pp. 14297–14306.
- Miao, N., H. Zhou, L. Mou, R. Yan, and L. Li (2019). Cgmh: Constrained sentence generation by metropolis-hastings sampling. In *Proceedings of the AAAI Conference on Artificial Intelligence*, Volume 33, pp. 6834–6842.
- Mnih, V., K. Kavukcuoglu, D. Silver, A. A. Rusu, J. Veness, M. G. Bellemare, A. Graves, M. Riedmiller, A. K. Fidjeland, G. Ostrovski, et al. (2015). Human-level control through deep reinforcement learning. *nature* 518(7540), 529–533.

- Mudgal, S., J. Lee, H. Ganapathy, Y. Li, T. Wang, Y. Huang, Z. Chen, H.-T. Cheng, M. Collins, T. Strohmaier, et al. (2023). Controlled decoding from language models. *arXiv preprint arXiv:2310.17022*.
- Nachum, O., M. Norouzi, K. Xu, and D. Schuurmans (2017). Bridging the gap between value and policy based reinforcement learning. *Advances in neural information processing systems* 30.
- Naesseth, C. A., F. Lindsten, T. B. Schön, et al. (2019). Elements of sequential monte carlo. *Foundations and Trends® in Machine Learning* 12(3), 307–392.
- Nakano, R., J. Hilton, S. Balaji, J. Wu, L. Ouyang, C. Kim, C. Hesse, S. Jain, V. Kosaraju, W. Saunders, et al. (2021). Webgpt: Browser-assisted question-answering with human feedback. *arXiv preprint arXiv:2112.09332*.
- Nisonoff, H., J. Xiong, S. Allenspach, and J. Listgarten (2024). Unlocking guidance for discrete state-space diffusion and flow models. *arXiv preprint arXiv:2406.01572*.
- Peng, X. B., A. Kumar, G. Zhang, and S. Levine (2019). Advantage-weighted regression: Simple and scalable off-policy reinforcement learning. *arXiv preprint arXiv:1910.00177*.
- Peters, J., K. Mulling, and Y. Altun (2010). Relative entropy policy search. In *Proceedings of the AAAI Conference on Artificial Intelligence*, Volume 24, pp. 1607–1612.
- Phillips, A., H.-D. Dau, M. J. Hutchinson, V. De Bortoli, G. Deligiannidis, and A. Doucet (2024). Particle denoising diffusion sampler. *arXiv preprint arXiv:2402.06320*.
- Podell, D., Z. English, K. Lacey, A. Blattmann, T. Dockhorn, J. Müller, J. Penna, and R. Rombach (2023). Sdxl: Improving latent diffusion models for high-resolution image synthesis. *arXiv preprint arXiv:2307.01952*.
- Prabhudesai, M., A. Goyal, D. Pathak, and K. Fragkiadaki (2023). Aligning text-to-image diffusion models with reward backpropagation. *arXiv preprint arXiv:2310.03739*.
- Qin, L., S. Welleck, D. Khoshdel, and Y. Choi (2022). Cold decoding: Energy-based constrained text generation with langevin dynamics. *Advances in Neural Information Processing Systems* 35, 9538–9551.
- Rector-Brooks, J., M. Hasan, Z. Peng, Z. Quinn, C. Liu, S. Mittal, N. Dziri, M. Bronstein, Y. Bengio, P. Chatterjee, et al. (2024). Steering masked discrete diffusion models via discrete denoising posterior prediction. *arXiv preprint arXiv:2410.08134*.
- Ren, Y., H. Chen, G. M. Rotskoff, and L. Ying (2024). How discrete and continuous diffusion meet: Comprehensive analysis of discrete diffusion models via a stochastic integral framework. *arXiv preprint arXiv:2410.03601*.
- Ren, Z., L. Jiang, Y. Di, D. Zhang, J. Gong, J. Gong, Q. Jiang, Z. Fu, P. Sun, B. Zhou, et al. (2024). Codonbert: a bert-based architecture tailored for codon optimization using the cross-attention mechanism. *Bioinformatics*, btae330.

- Rombach, R., A. Blattmann, D. Lorenz, P. Esser, and B. Ommer (2022). High-resolution image synthesis with latent diffusion models. In *Proceedings of the IEEE/CVF conference on computer vision and pattern recognition*, pp. 10684–10695.
- Ross, S. and D. Bagnell (2010). Efficient reductions for imitation learning. In *Proceedings of the thirteenth international conference on artificial intelligence and statistics*, pp. 661–668. JMLR Workshop and Conference Proceedings.
- Ross, S., G. Gordon, and D. Bagnell (2011). A reduction of imitation learning and structured prediction to no-regret online learning. In *Proceedings of the fourteenth international conference on artificial intelligence and statistics*, pp. 627–635. JMLR Workshop and Conference Proceedings.
- Rusu, A. A., S. G. Colmenarejo, C. Gulcehre, G. Desjardins, J. Kirkpatrick, R. Pascanu, V. Mnih, K. Kavukcuoglu, and R. Hadsell (2015). Policy distillation. *arXiv preprint arXiv:1511.06295*.
- Sahoo, S. S., M. Arriola, Y. Schiff, A. Gokaslan, E. Marroquin, J. T. Chiu, A. Rush, and V. Kuleshov (2024). Simple and effective masked diffusion language models. *arXiv preprint arXiv:2406.07524*.
- Salimans, T. and J. Ho (2022). Progressive distillation for fast sampling of diffusion models. *arXiv preprint arXiv:2202.00512*.
- Salomon-Ferrer, R., D. A. Case, and R. C. Walker (2013). An overview of the amber biomolecular simulation package. *Wiley Interdisciplinary Reviews: Computational Molecular Science* 3(2), 198–210.
- Saremi, S. and A. Hyvärinen (2019). Neural empirical bayes. *Journal of Machine Learning Research* 20(181), 1–23.
- Sarkar, A., Z. Tang, C. Zhao, and P. Koo (2024). Designing dna with tunable regulatory activity using discrete diffusion. *bioRxiv*, 2024–05.
- Schuhmann, C. (2022, Aug). LAION aesthetics.
- Schulman, J., S. Levine, P. Abbeel, M. Jordan, and P. Moritz (2015). Trust region policy optimization. In *International conference on machine learning*, pp. 1889–1897. PMLR.
- Schulman, J., F. Wolski, P. Dhariwal, A. Radford, and O. Klimov (2017). Proximal policy optimization algorithms. *arXiv preprint arXiv:1707.06347*.
- Seo, S., M. Kim, T. Shen, M. Ester, J. Park, S. Ahn, and W. Y. Kim (2024). Generative flows on synthetic pathway for drug design. *arXiv preprint arXiv:2410.04542*.
- Shi, J., K. Han, Z. Wang, A. Doucet, and M. K. Titsias (2024). Simplified and generalized masked diffusion for discrete data. *arXiv preprint arXiv:2406.04329*.
- Silver, D., A. Huang, C. J. Maddison, A. Guez, L. Sifre, G. Van Den Driessche, J. Schrittwieser, I. Antonoglou, V. Panneershelvam, M. Lanctot, et al. (2016). Mastering the game of go with deep neural networks and tree search. *nature* 529(7587), 484–489.

- Singhal, R., Z. Horvitz, R. Teehan, M. Ren, Z. Yu, K. McKeown, and R. Ranganath (2025). A general framework for inference-time scaling and steering of diffusion models. *arXiv preprint arXiv:2501.06848*.
- Sohl-Dickstein, J., E. Weiss, N. Maheswaranathan, and S. Ganguli (2015). Deep unsupervised learning using nonequilibrium thermodynamics. In *International conference on machine learning*, pp. 2256–2265. PMLR.
- Song, J., C. Meng, and S. Ermon (2020). Denoising diffusion implicit models. *arXiv preprint arXiv:2010.02502*.
- Song, J., A. Vahdat, M. Mardani, and J. Kautz (2023). Pseudoinverse-guided diffusion models for inverse problems. In *International Conference on Learning Representations*.
- Song, Y., P. Dhariwal, M. Chen, and I. Sutskever (2023). Consistency models. *arXiv preprint arXiv:2303.01469*.
- Song, Y. and S. Ermon (2019). Generative modeling by estimating gradients of the data distribution. *Advances in neural information processing systems* 32.
- Song, Y., J. Sohl-Dickstein, D. P. Kingma, A. Kumar, S. Ermon, and B. Poole (2021). Score-based generative modeling through stochastic differential equations. *ICLR*.
- Stanton, D. T. and P. C. Jurs (1990). Development and use of charged partial surface area structural descriptors in computer-assisted quantitative structure-property relationship studies. *Analytical Chemistry* 62(21), 2323–2329.
- Sun, H., L. Yu, B. Dai, D. Schuurmans, and H. Dai (2022). Score-based continuous-time discrete diffusion models. *arXiv preprint arXiv:2211.16750*.
- Sun, W., D. Chen, C. Wang, D. Ye, Y. Feng, and C. Chen (2023). Accelerating diffusion sampling with classifier-based feature distillation. In *2023 IEEE International Conference on Multimedia and Expo (ICME)*, pp. 810–815. IEEE.
- Sun, W., A. Venkatraman, G. J. Gordon, B. Boots, and J. A. Bagnell (2017). Deeply aggregated: Differentiable imitation learning for sequential prediction. In *International conference on machine learning*, pp. 3309–3318. PMLR.
- Swanson, K., G. Liu, D. B. Catacutan, A. Arnold, J. Zou, and J. M. Stokes (2024). Generative ai for designing and validating easily synthesizable and structurally novel antibiotics. *Nature Machine Intelligence* 6(3), 338–353.
- Tang, W. and H. Zhao (2024). Score-based diffusion models via stochastic differential equations—a technical tutorial. *arXiv preprint arXiv:2402.07487*.
- Trippe, B. L., J. Yim, D. Tischer, D. Baker, T. Broderick, R. Barzilay, and T. Jaakkola (2022). Diffusion probabilistic modeling of protein backbones in 3d for the motif-scaffolding problem. *arXiv preprint arXiv:2206.04119*.

- Trott, O. and A. J. Olson (2010). Autodock vina: improving the speed and accuracy of docking with a new scoring function, efficient optimization, and multithreading. *Journal of computational chemistry* 31(2), 455–461.
- Uehara, M., Y. Zhao, T. Biancalani, and S. Levine (2024). Understanding reinforcement learning-based fine-tuning of diffusion models: A tutorial and review. *arXiv preprint arXiv:2407.13734*.
- Uehara, M., Y. Zhao, K. Black, E. Hajiramezanali, G. Scalia, N. L. Diamant, A. M. Tseng, T. Biancalani, and S. Levine (2024). Fine-tuning of continuous-time diffusion models as entropy-regularized control. *arXiv preprint arXiv:2402.15194*.
- Uehara, M., Y. Zhao, K. Black, E. Hajiramezanali, G. Scalia, N. L. Diamant, A. M. Tseng, S. Levine, and T. Biancalani (2024, 21–27 Jul). Feedback efficient online fine-tuning of diffusion models. In R. Salakhutdinov, Z. Kolter, K. Heller, A. Weller, N. Oliver, J. Scarlett, and F. Berkenkamp (Eds.), *Proceedings of the 41st International Conference on Machine Learning*, Volume 235 of *Proceedings of Machine Learning Research*, pp. 48892–48918. PMLR.
- Uehara, M., Y. Zhao, E. Hajiramezanali, G. Scalia, G. Eraslan, A. Lal, S. Levine, and T. Biancalani (2024). Bridging model-based optimization and generative modeling via conservative fine-tuning of diffusion models. In *The Thirty-eighth Annual Conference on Neural Information Processing Systems*.
- Venkatraman, S., M. Jain, L. Scimeca, M. Kim, M. Sendera, M. Hasan, L. Rowe, S. Mittal, P. Lemos, E. Bengio, et al. (2024). Amortizing intractable inference in diffusion models for vision, language, and control. *arXiv preprint arXiv:2405.20971*.
- Vignac, C., I. Krawczuk, A. Siraudin, B. Wang, V. Cevher, and P. Frossard (2023). Digress: Discrete denoising diffusion for graph generation. In *The Eleventh International Conference on Learning Representations*.
- Vincent, P. (2011). A connection between score matching and denoising autoencoders. *Neural computation* 23(7), 1661–1674.
- Wang, A. and K. Cho (2019). Bert has a mouth, and it must speak: Bert as a markov random field language model. *arXiv preprint arXiv:1902.04094*.
- Wang, C., M. Uehara, Y. He, A. Wang, T. Biancalani, A. Lal, T. Jaakkola, S. Levine, H. Wang, and A. Regev (2024). Fine-tuning discrete diffusion models via reward optimization with applications to dna and protein design. *arXiv preprint arXiv:2410.13643*.
- Wang, X., Z. Zheng, F. Ye, D. Xue, S. Huang, and Q. Gu (2024). Dplm-2: A multimodal diffusion protein language model. *arXiv preprint arXiv:2410.13782*.
- Watson, J. L., D. Juergens, N. R. Bennett, B. L. Trippe, J. Yim, H. E. Eisenach, W. Ahern, A. J. Borst, R. J. Ragotte, L. F. Milles, et al. (2023). De novo design of protein structure and function with rfdiffusion. *Nature* 620(7976), 1089–1100.
- Widatalla, T., R. Rafailov, and B. Hie (2024). Aligning protein generative models with experimental fitness via direct preference optimization. *bioRxiv*, 2024–05.

- Winnifrieth, A., C. Outeiral, and B. L. Hie (2024). Generative artificial intelligence for de novo protein design. *Current Opinion in Structural Biology* 86, 102794.
- Wu, L., B. Trippe, C. Naesseth, D. Blei, and J. P. Cunningham (2024). Practical and asymptotically exact conditional sampling in diffusion models. *Advances in Neural Information Processing Systems* 36.
- Xiao, C., R. Huang, J. Mei, D. Schuurmans, and M. Müller (2019). Maximum entropy monte-carlo planning. *Advances in Neural Information Processing Systems* 32.
- Xu, M., L. Yu, Y. Song, C. Shi, S. Ermon, and J. Tang (2022). Geodiff: A geometric diffusion model for molecular conformation generation. *arXiv preprint arXiv:2203.02923*.
- Yang, K. and D. Klein (2021). Fudge: Controlled text generation with future discriminators. *arXiv preprint arXiv:2104.05218*.
- Yang, X., T. K. Aasawat, and K. Yoshizoe (2020). Practical massively parallel monte-carlo tree search applied to molecular design. *arXiv preprint arXiv:2006.10504*.
- Yang, X., J. Zhang, K. Yoshizoe, K. Terayama, and K. Tsuda (2017). Chemts: an efficient python library for de novo molecular generation. *Science and technology of advanced materials* 18(1), 972–976.
- Yap, C. W. (2011). Padel-descriptor: An open source software to calculate molecular descriptors and fingerprints. *Journal of computational chemistry* 32(7), 1466–1474.
- Ye, F., Z. Zheng, D. Xue, Y. Shen, L. Wang, Y. Ma, Y. Wang, X. Wang, X. Zhou, and Q. Gu (2024). Proteinbench: A holistic evaluation of protein foundation models. *arXiv preprint arXiv:2409.06744*.
- Yim, J., B. L. Trippe, V. De Bortoli, E. Mathieu, A. Doucet, R. Barzilay, and T. Jaakkola (2023). Se (3) diffusion model with application to protein backbone generation. *arXiv preprint arXiv:2302.02277*.
- Yuan, H., K. Huang, C. Ni, M. Chen, and M. Wang (2024). Reward-directed conditional diffusion: Provable distribution estimation and reward improvement. *Advances in Neural Information Processing Systems* 36.
- Zhang, L., A. Rao, and M. Agrawala (2023). Adding conditional control to text-to-image diffusion models. In *Proceedings of the IEEE/CVF International Conference on Computer Vision*, pp. 3836–3847.
- Zhang, R., M. Haider, M. Yin, J. Qiu, M. Wang, P. Bartlett, and A. Zanette (2024). Accelerating best-of-n via speculative rejection.
- Zhao, S., R. Brekelmans, A. Makhzani, and R. Grosse (2024). Probabilistic inference in language models via twisted sequential monte carlo. *arXiv preprint arXiv:2404.17546*.
- Zhao, Y., J. Shi, L. Mackey, and S. Linderman (2024). Informed correctors for discrete diffusion models. *arXiv preprint arXiv:2407.21243*.

Zhao, Y., M. Uehara, G. Scalia, T. Biancalani, S. Levine, and E. Hajiramezanali (2024). Adding conditional control to diffusion models with reinforcement learning. *arXiv preprint arXiv:2406.12120*.